inorganics

MDPI

Review

Recent Advances in Lanthanide Metal–Organic Framework Thin Films Based on Eu, Tb, Gd: Preparation and Application as Luminescent Sensors and Light-Emitting Devices

Helena Brunckova *, Erika Mudra and Ivan Shepa

Institute of Materials Research, Slovak Academy of Sciences, Watsonova 47, 040 01 Kosice, Slovakia; emudra@saske.sk (E.M.); ishepa@saske.sk (I.S.)

* Correspondence: hbrunckova@saske.sk; Tel.: +421-55-7922-455

Abstract: Lanthanide Metal–Organic Frameworks (LnMOFs), in recent years, have developed into an interesting subclass of MOFs. While the number of published papers, in particular, were dedicated to their synthesis and functional properties, along with the application mechanisms of MOFs, only a few of them have been focused on LnMOFs thin films independently. LnMOFs have become interesting thanks to their outstanding properties, for example, excellent structural flexibility, tunable pore size, surface area, functionality, and good chemical stability. Significant progress over the past two decades in the preparation of MOF films has been achieved, especially towards the development of green, or at least greener, synthesis approaches. We begin with insight into various types of MOFs and summarize recent achievements in the production of LnMOF films, along with various film preparation approaches. Afterward, we briefly discuss the applications of luminescence features of lanthanide ions in films and their potential as white-light source materials. We also covered films based on Eu, Tb, and Gd with particular accents on different design approaches. Moreover, specifically, luminescent features applied for sensing temperature, a variety of ions, gases, and biomolecules are highlighted. The review ends with a comprehensive conclusion about the state-of-art-potential of LnMOFs together with an outlook on the future of LnMOF films in future technologies.

Keywords: metal–organic frameworks; lanthanide; preparation; luminescent sensors; thin films

Citation: Brunckova, H.; Mudra, E.; Shepa, I. Recent Advances in Lanthanide Metal–Organic Framework Thin Films Based on Eu, Tb, Gd: Preparation and Application as Luminescent Sensors and Light-Emitting Devices. *Inorganics* **2023**, *11*, 376. https://doi.org/10.3390/inorganics11100376

Academic Editor: Christian Julien

Received: 1 September 2023
Revised: 20 September 2023
Accepted: 21 September 2023
Published: 23 September 2023

1. Introduction

Porous coordination polymers, commonly known as Metal–Organic Frameworks, or simply MOFs, are crystalline nanoporous materials, formed by metal ions or metal-containing clusters bonded by organic linkers, which form various dimensional structures [1–5]: two-dimensional (2D) [6,7] or three-dimensional (3D) extended network [8–11]. Metal ions of the first-row transition series, such as Cr^{3+}, Fe^{3+}, Co^{2+}, and Zn^{2+}, are commonly used as connectors for the formation of MOFs [9]. Thanks to high structural flexibility, large surface area, along with tunable pore size, MOFs have applications in the fields of gas sorption [12], separation and storage [13,14], catalysis [15,16], molecular recognition and sensing [17,18], drug delivery [19], and luminescence and non-linear optics [2,9]. The recently developed subclass of Metal–Organic Frameworks, known as luminescent MOFs (LMOFs), show promise for use as light-emitting materials due to their crystalline structure and unique optical properties [20]. However, the application of LMOFs is not limited only to luminophores. Luminescent properties pave the way for such MOF materials in the sensing field as biosensors thanks to low biotoxicity and easy preparation in the form of thin films (TFs) [21].

Lanthanide (Ln) ions are known for their high coordination numbers and diverse coordination geometry, which sets them apart from transition metal ions [22,23]. This has led to a surge of interest in Lanthanide-based Metal-Organic Frameworks (LnMOFs), a subset of Luminescent MOFs (LMOFs). The exceptional luminescent characteristics of

Ln ions, including large Stokes shifts, distinct sharp emissions, extended lifetime, and color purity with high quantum yields in both the near-infrared and visible regions, make LnMOFs particularly intriguing [5,8,24–26]. In addition, LnMOFs are known for their features, such as varied topology, modifiable structure, porosity, and surface area. However, it is important to note that the luminescent attributes of Ln ions are significantly influenced by the structure of their surrounding coordination environment. This makes them a fascinating and promising platform for use in chemical sensors [27–31]. The integration of Ln ions' properties with the topological attributes of MOFs paves the way for the creation of new luminescent materials. These could potentially be used in white light sources, such as Light Emitting Diodes (LEDs) [20,32–34]. Thanks to the narrow absorption cross-section and limited absorption efficiency of Ln ions and due to the parity-forbidden f-f transitions, it is still difficult to yield strong luminescence through the direct photoexcitation of Ln ions. However, this task can be achieved via energy transfer processes, known as "luminescence sensitization" or the "antenna effect" [21,24,26,35]. The "antenna effect" is based on the property of organic ligands to act as an antenna—by absorbing completely optical energy and then transferring it to the coordinated central Ln ions through a molecular energy transfer mode. Single-Ln^{3+} in LnMOFs demonstrate a basic luminescent behavior. On the other hand, mixed-Ln^{3+} in LnMOFs display a remarkable capability for adjustable white light emission and temperature gauging [4,26].

LnMOF-TFs are gaining prominence in various application areas, including optoelectronics, gas separation, catalysis electronic devices, and biomedicine. Thin films, compared to solution-based powdery substances, offer several unique benefits, such as excellent stability and portability, adjustable shape and size, real-time detection, non-invasiveness, and broad applicability in gas/vapor sensing and recycling [2]. The luminescence of MOF-TFs can be derived from luminescent metal ions or clusters, organic ligands, loaded guest molecules, and charge transfer: either ligand-to-metal or the reverse—metal-to-ligand [21]. Mixed-crystal LnMOFs (Ln = Eu + Tb, Eu + Tb + Gd) [36], TFs, as opposed to the traditional method based on single lanthanide ions [36–38], produce more stable and precise luminescent signals. This makes them an excellent choice for self-calibrating luminescent sensors for a variety of applications [39,40]. Again, compared to sensors that contain only one luminescent site, the mixed-crystal LnMOFs with a self-referring strategy can amplify the relative emission ratios, which would improve the luminescent signals and decoding of the analyzed molecules [40,41]. In the case of films, di- or higher-topic organic linkers can be employed to act as light-absorbing antennae [42,43]. Films exhibit permanent porosity and have been utilized for numerous applications, including tunable emission, biosensing [44], and thermometers [45–47].

It is of great significance to prepare high-quality LnMOF TFs with precise control over the thickness, morphology, density, crystallinity, roughness, and orientation [5]. Various hydro/solvothermal, sonochemical, microwave-assisted, and electrochemical synthetic strategies are available [4,5]. The deposition of high-quality LnMOF-TFs is still challenging but offers potential applications in gas storage, catalysis, sensing, lighting, and solar energy harvesting [48]. Many methods have been developed for film deposition: directly onto bare substrates or functionalized substrates with organic molecules [49]; on seeded substrates; on preformed MOF nanocrystals; layer by layer [50–52]; and electrodeposition [5,46]. Silicon wafers, glass, indium tin oxide (ITO), fluoride tin oxide (FTO), and porous aluminum oxide are mostly used as substrates for LnMOF films [46]. Because of the excellent detection performance and the turnability of light emission, lanthanide composite hybrid films have drawn a lot of attention in recent years [32,53–55]. Processing methods that enable the creation of either pure luminescent materials with specific shape and structure under certain conditions, or hybrid materials on designated substrates, are of great interest [10]. MOFs are often considered among the top luminescent materials due to their multiple fluorescent mechanisms, such as ligand-centered emission and guest-centered emission [34]. LnMOF-TFs represent a promising category of porous crystalline materials that can be customized for various practical applications through versatile post-synthetic modifications [56]. Primarily, the

introduction of lanthanide ions can bring to life their native optical and photonic properties. Metal-centered luminescence is commonly observed in Ln-FMOFs. The f-f transitions of lanthanide ions (Ln^{3+}) are parity-forbidden but can be sensitized by organic ligands through a process known as the "antenna effect" [56].

There are already several excellent reviews published [3–5,8,21,57–59] focusing on the fabrication of LnMOF films, which also include the idea of mixed matrix membranes [60–63]. This is why the present work aims to comprehensively describe the current progress in the preparation of MOF-TFs, with a particular focus on those that are the lanthanide-based, and the green synthesis of LnMOFs as light-emitting materials [20,26] and chemical sensors with single and/or multiple luminescent centers [64]. A brief perspective of the application of LnMOFs in light-emitting devices is presented and classified from the viewpoint of the general luminescence features of LnMOFs. The potential of LnMOFs for sensing applications is overviewed toward the detection of a variety of anions, cations, nitroaromatic, and other small molecules in the form of vapors and/or gases.

2. Preparation Methods of LnMOF-TFs

The previously published reviews were mostly focused on the existing and potential applications, as well as the synthesis methods of MOF-TFs [3,5,8,65]. However, regarding the fabrication approaches, these reviews focused mostly on hydro/solvothermal (HT/ST) synthesis, layer-by-layer (LBL) deposition, and electrochemical depositions. According to [5,25], five types of MOF-TFs can be distinguished based on their production:

1. Casted MOF-TFs—solvothermally synthesized nanocrystalline powders are cast onto a pretreated substrate;
2. SURMOFs—Surface-supported Metal–Organic Frameworks—fabricated using the layer-by-layer method, where the orientation and film thickness can be easily and precisely controlled;
3. Electrochemically (electrophoretically) deposited MOF films;
4. Ultrasonic spray-deposited MOF;
5. MOF-TFs made by using vapor–solid synthesis—ALD/MLD.

For the mentioned techniques, depending on the planned composition and particular applications, the host surface/deposition substrates, usually Si, Zn, ITO, FTO, and Al_2O_3, were used. Taking into account the discussed publications on MOFs in the forms of membranes [62], composite structures [66], and free-standing nanoparticles (NPs) [67], moving forward, the authors will concentrate on the production of Metal–Organic Framework Thin Films (MOF-TFs). They will provide an exhaustive review of the various synthesis strategies for MOF-TFs, including patterns, and will discuss potential directions for future advancements and environmentally friendly fabrication.

2.1. Solvo/Hydrothermal Deposition

The solvothermal growth of films is a simple, effective, and low-cost deposition method that has been widely accepted [5]. The disadvantage of conventional synthesis is the high cost due to the large organic reactants consumption and waste production [8]. Green modulation synthesis is used for the preparation of nano-sized LnMOFs using eco-friendly chemicals.

2.1.1. In Situ Direct Growth

In situ, the direct deposition of the LnMOF, Ln-BTC, and mixed-crystal Ln-BTC films can be easily realized on bare (1) and modified (2) substrates. Both approaches are visualized in Figure 1. Nanometer-sized MOF-TFs (NMOFs) were prepared on indium–tin oxide (ITO) glass using a solution of Ln^{3+} in DMF/H_2O or EtOH/H_2O mixed with sodium acetate (NaOAc) as modulator and followed by spin-coating (SC) or dip-coating (DC) without any substrate modification. As a result, two smooth continuous films were reported: $Eu_{0.5}Tb_{0.5}$-BTC by SC [68], Tb-BTC by DC [69] and $Eu_{0.1}Tb_{0.9}$-BTC (MILMOF-3) by DC [40]. A series of reticular Ln-BTC, where Ln = Eu, Gd, and Tb, were directly grown on cotton

fibers using a room-temperature water-based direct precipitation method [70]. The one-step direct solvothermal synthesis of LnMOF film is reported for the LnHL, $Gd_{0.9}Tb_{0.1}HL$ (H_4L = 5-hydroxy-1,2,4-benzenetricarboxylic acid) continuous and smooth films that were deposited on Gd_2O_3 substrate [46]. For the first time, LnMOF-TFs were created using an in situ direct solvothermal method on a Gd_2O_3 substrate. The surface Gd ions from the Gd_2O_3 substrate not only aid in the formation, but also enhance the quality of the film by serving as nucleation sites for the growth of an LnMOF [46].

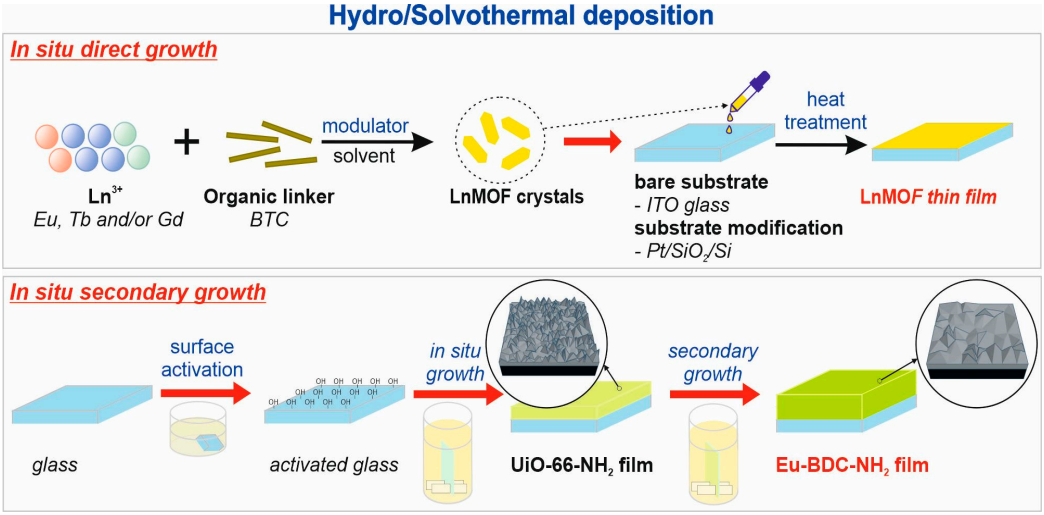

Figure 1. Schematic depiction of hydro/solvothermal in situ direct growth of LnMOFs (Ln-BTC) on ITO glass or $Pt/SiO_2/Si$ substrates, and the in situ secondary growth of Eu-BDC-NH_2 film on activated glass with UIO-66-NH_2 as a seed layer. The figures were recreated and adapted from those presented in [40,71–73].

Solvothermal synthesis (ST) is a kind of chemical synthesis performed in the liquid state in a non-aqueous solvent media at relatively high temperatures and pressures. It is realized in an enclosed vessel, heated up above the boiling point of the liquid media, which results in the pressure rise. Hydrothermal synthesis (HT) refers to solvothermal synthesis, in which the solvent used is water [8,74]. In typical hydro/solvothermal syntheses, the desired substrate is placed in a solution or mixture of precursors and is subjected to a reaction at a high temperature. As a result, the formed solid phase is even deposited and distributed on the surface of the substrate. The hydro/solvothermal growth of MOF-TFs is simple in preparation, feasible, efficient, and well reproducible deposition method and thus is commonly used for the production of electronic and optoelectronic devices [75]. A walkthrough of the general process step by step is depicted in Figure 1, in which upon heating, LnMOFs growth occurs rapidly on the substrate: bare—ITO glass—Eu/Tb-BTC film [40], one modified with platinum layer on SiO_2/Si wafer—Tb-BTC, $Eu_{0.25}Gd_{0.5}Tb_{0.25}$-BTC films, [71,72,76] and one with a seed layer of a UiO-66-NH_2—Eu-BDC-NH_2 film [73]. The XRD data of Ln-BTC films are in good agreement with the tetragonal structure P_4322 space group similar to Y(BTC)(H_2O) [40,71]. The XRD peaks of the Eu-BDC-NH_2 film slightly shifted to a lower degree compared to that of UiO-66-NH_2, which is mainly attributed to the larger ion size of Eu^{3+} compared to the Zr^{4+} [73].

Both the Tb-BTC crystalline (cTbMOF) and amorphous (aTbMOF) films were successfully prepared by solvothermal synthesis simply by changing the amount of NaOAc modulator used, that is, 0.4 and 0.7 mmol, respectively, according to our previous work [71]. The results of the syntheses are presented in Figure 2. Both crystalline and amorphous precursor solutions were prepared similarly from $Tb(NO_3)_3 \cdot 6H_2O$, the mixture of DMF/H_2O/NaOAc, and as follows, dropped on the surface of the SiO_2/Si substrates modified by the deposited platinum interlayer. SEM and AFM micrographs of crystalline and amorphous films are

presented in Figure 2. As shown in Figure 2a, particles of crystalline TbBTC powder with an average size of 300 nm (observed by TEM), were obtained with the use of a 0.4 mmol NaOAc modulator [71]. The SEM micrographs of cTbMOF (Figure 2b) reveal a straw-sheaf-like structure, which is in agreement with that reported in the literature [71]. The porous crystalline film of the synthesized MOF consists of needle-like particles with a variety of elongated shapes of 80–150 nm in size. The isometric AFM micrographs show that the topography of the cTbMOF-TF (Figure 2c) film is formed by the uniform clusters of particles, while the average surface roughness (Sa) of the film was evaluated as 42.1 nm for the 1 μm × 1 μm area. Amorphous aTbMOF powder was obtained when the amount of NaOAc was increased up to 0.7 mmol (Figure 2d). The HR-TEM micrographs reveal no lattice fringes, confirming its amorphous nature. The SEM image of the MOF film reveals that the surface of the samples has become quite uneven (Figure 2e). The SEM image distinctly illustrates the macroporous structure of the fabricated MOF, which is composed of worm-like nanoparticles that are approximately 100 nm in diameter. In Figure 2f, the surface roughness for the amorphous aTbMOF-TF is higher—58.1 nm—compared to the cMOF film for the same scan size.

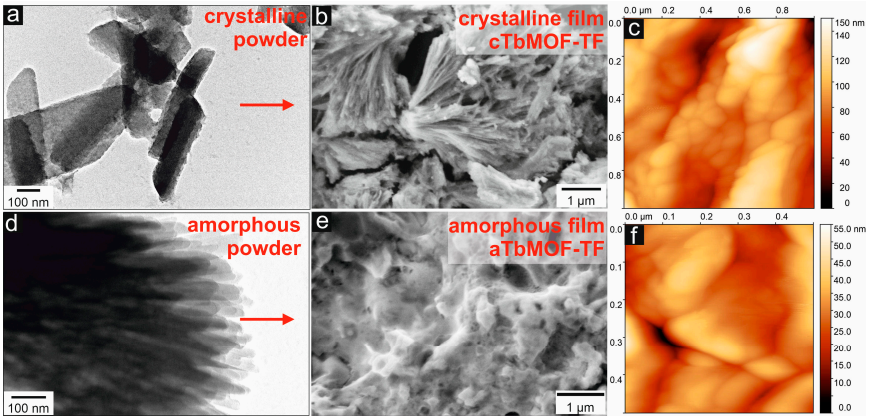

Figure 2. TEM images of Tb-BTC powders: (**a**) crystalline and (**d**) amorphous. SEM and 2D AFM images of TbMOF-TF thin films: (**b**,**c**) crystalline and (**e**,**f**) amorphous.

Similarly to the film described in [71], porous transparent mixed Ln-BTC films, where Ln = Eu/Gd/Tb, with a thickness of ~0.5–1.2 μm, were prepared on modified $Pt/SiO_2/Si$ substrates from nanocrystals via green solvothermal synthesis using a mixture of $EtOH/H_2O$/NaOAc as a solvent [72]. Three different ratios of lanthanides are chosen for the preparation of mixed LnMOFs films with the bi-doped concentration of Eu^{3+}/Tb^{3+} ions in Gd-BTC. Figure 3 shows the FTIR spectra of LnMOF (Ln-BTC, Ln = Eu, Gd, Tb, $Eu_{0.25}Gd_{0.5}Tb_{0.25}$) powders. In the spectra (Figure 3a), the wide peak at 3435 cm^{-1} is assigned to the ν(OH) groups. The effect of acetate groups from sodium acetate on LnMOF can be noticed in the regions at 2995, 2780, and 2430 cm^{-1}, which are assigned to stretching ν(C-H) vibrations. In the spectra, the bands in zones 1560–1520 cm^{-1} and 1385 cm^{-1} were marked as stretching vibrations of the COO^- groups ν_{as} and ν_s, respectively. The bands of corresponding COOH groups designate the complete deprotonation of the carboxylic acid and the coordination of COO^- groups to the lanthanide center. The peak that appeared at 565 cm^{-1} can be assigned to the stretching vibration of Ln-O. Figure 3b shows the XRD patterns for both samples (powder and film). For TbMOF powder, the results were compared with the crystallographic data in the Cambridge Database (CIF no. 617492 for Tb-BTC); the match confirms the expected tetragonal phase for Tb-BTC [71]. Similar to the XRD of crystalline powder, the $Eu_{0.25}Gd_{0.5}Tb_{0.25}$MOF film reveals peaks at 10.5, 11.5, 16.1, 21.3, and 29.3° (2θ), and Pt and Si peaks from the substrate. In Figure 3c, the photographs of prepared TbMOF powders and various films (TbMOF and EuGdTbMOF) on $Pt/SiO_2/Si$ substrate were shown. In Figure 3, the TEM morphology of mixed lanthanide LnMOF powder along with SEM microstructure and AFM topography of mixed $Eu_{0.25}Gd_{0.5}Tb_{0.25}$-BTC

are depicted. As shown in Figure 3d, particles of crystalline MOF powder with an average size of 50–100 nm were confirmed by TEM. In Figure 3e, it is visible that the surface of the film is formed by lace-like and ribbon-like structures with a size of 50–120 nm, which were consistent with MOF particles. In addition, some MOF crystals exhibit an elongated hexagonal morphology of 80–120 nm in size. The thickness of the dense continuous film is estimated to be approximately 1.0 µm. A similar growth mechanism of nano rod-like structures was recorded in LnMOF film on ITO substrate [40,69]. Figure 3f shows AFM images of the film prepared by the green method. The surface roughness value (Sa) of the film was measured as 45.2 nm for a 1 µm × 1 µm image. The AFM images illustrate that the average particle size is about 100–300 nm and corresponds to the size of particles in the film estimated from the SEM micrographs in Figure 3e.

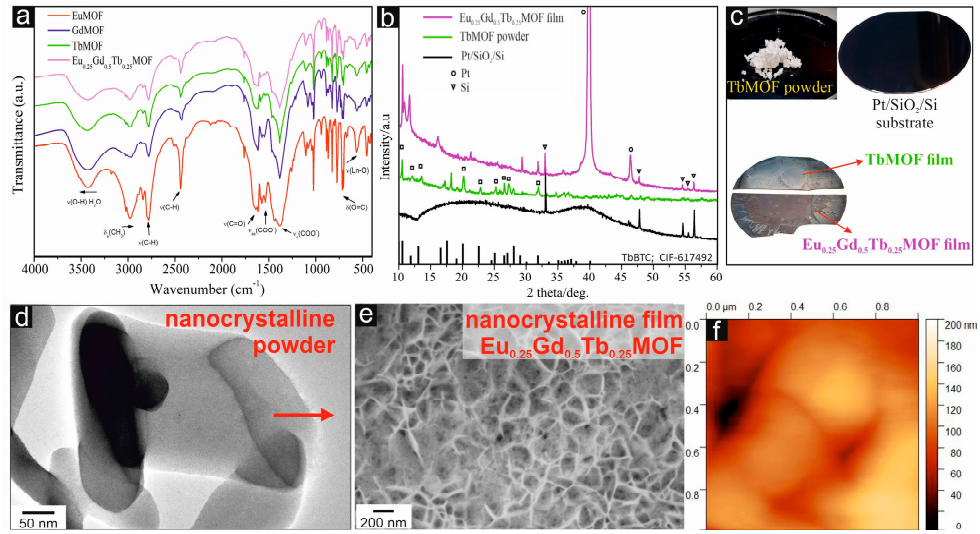

Figure 3. (**a**) FTIR spectra, (**b**) XRD, and (**c**) photos of LnMOF powders and thin films; (**d**) TEM, (**e**) SEM, and (**f**) isometric AFM micrographs of $Eu_{0.25}Gd_{0.5}Tb_{0.25}$MOF thin film prepared by green hydrothermal synthesis.

2.1.2. In Situ Secondary Growth

Zhang and colleagues pioneered a novel technique called "in situ secondary growth" for the fabrication of lanthanide MOF films [73]. They successfully utilized this method to create a Eu-BDC-NH_2 film on ordinary glass, using UiO-66-NH_2 as the seed layer. This was achieved by leveraging the matching structure and components of the materials. This process is depicted in Figure 1. The "in situ secondary growth" strategy is a versatile method that can be extended to other lanthanide MOFs by selecting appropriate seed layers. The Eu-BDC-NH2 film exhibited strong characteristics of Eu^{3+} ion and was employed for the first time in the fluorescence sensing of gaseous SO_2 [73].

2.2. Layer-by-Layer Deposition

The layer-by-layer (LBL) assembly method involves the in situ growth of Metal–Organic Frameworks (MOFs) on various substrates. This process involves repeated cycles of immersing the substrate into a solution-source of metal ions and a solution-source of organic ligands [77–80]. Typically, the substrate is modified with a self-assembled monolayer (SAM), such as an organic linking molecule or metal oxide film. The thickness of the film can be effectively controlled by the number of growth cycles. While the LBL method offers several benefits, such as well-controlled thickness, surface roughness, and mild reactions at room temperature. It also has some drawbacks, including the need for repeated operations and lengthy reaction times [5,8].

A continuous and well-adhered thin film of EuMOF—Eu-NDC@HPAN, exhibiting dual-emission was directly cultivated on hydrolyzed polyacrylonitrile (HPAN) using the

layer-by-layer (LBL) method [81]. This film was employed as a self-calibrating luminescent sensor for the detection of formaldehyde in aqueous media. Silk fiber was used as the framework for the successful coating of the dense luminescent MOF-76(Tb), Tb-BTC, forming a composite MOF-76(Tb)@silk fiber using the LBL method [82]. The prepared composite is a prospective candidate for the detection of aquatic Cu^{2+}. In the typical LBL MOF preparation [82], precursor solution 1 consists of Tb^{3+}, DMF, EtOH, and H_2O. Precursor solution 2 is a mixture of H_3BTC, DMF, EtOH, and H_2O. The silk fibers were dipped in solutions 1 and 2 for 4 h, alternatively. After each dipping, the silk fiber was rinsed in ethanol to remove the unreacted precursor. The results of such preparation are shown in Figure 4.

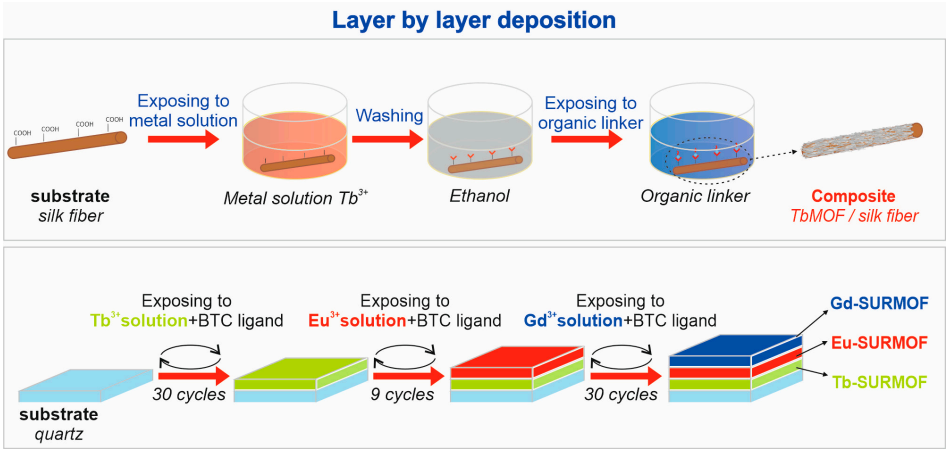

Figure 4. Schematic representation of the layer-by-layer method used for the preparation of Tb-BTC-coated silk fibers as MOF-76(Tb)@silk fiber composite (upper part) and Ln-SURMOF film as triple (Tb, Eu, Gd) layers on a quartz substrate (lower part). Adapted from [82,83].

Chen et al. [83,84] prepared a new set of films using LBL, known as Ln-SURMOFs (surface-supported MOFs), to produce solid-state white light-emitting devices. The thickness of the transparent multicomponent, mixed Eu/Tb Ln-SURMOFs can be freely controlled. For example, it was reported that Eu-BTC was successfully grown epitaxially on the surface of a Tb-BTC SURMOF [84]. A three-component approach is similarly developed for the combination of red, green, and blue (RGB)-light-emitting Eu^{3+}-, Tb^{3+}-, and Gd^{3+}-containing layers to achieve the combined white light emission [83]. For the preparation of the triple-layer Tb/Eu/Gd-SURMOF multistage process a combination of three single-layer Ln-SURMOF depositions was adopted. (1) Tb-SURMOF was deposited on quartz substrate by LbL growth: the substrates were immersed into a solution of $Tb(NO_3)_3$ in ethanol for 12 min and then rinsed with pure ethanol; in the next step, the quartz substrates were immersed in an ethanolic solution of H_3BTC for 12 min and rinsed with pure ethanol again. This sequence was repeated for 30 cycles. (2) Similar Eu-SURMOF LbL growth was repeated from 4 to 9 cycles with the use of $Eu(NO_3)_3$ and H_3BTC. And (3) a Gd-SURMOF layer was grown on top of the device employing the same conditions as the Eu and Tb layers, but for 30 repetitions (Figure 4). The XRD data of the Ln-SURMOFs reveal the presence of highly crystalline oriented films with a sharp diffraction peak at 8.52° (2θ) [83].

2.3. Electrochemical Deposition

In comparison to the high temperature (HT) and solvothermal (ST) methods, electrochemical deposition (ECD) offers several benefits for the fabrication process of MOF-TFs [8,85–89]. These include a shorter growth time and the affordability of the required equipment. The continuous production process makes it appealing for industrial use, particularly for mass production. The reaction process is more controllable and reproducible. However, there are relatively few studies on lanthanide MOF thin films prepared using the ECD method [85–89] (Figure 5). This method does have some limitations that restrict its

application, such as challenges in growth control. The preparation of MOF films requires large quantities of chemicals and solvents, which can lead to environmental pollution and increased costs.

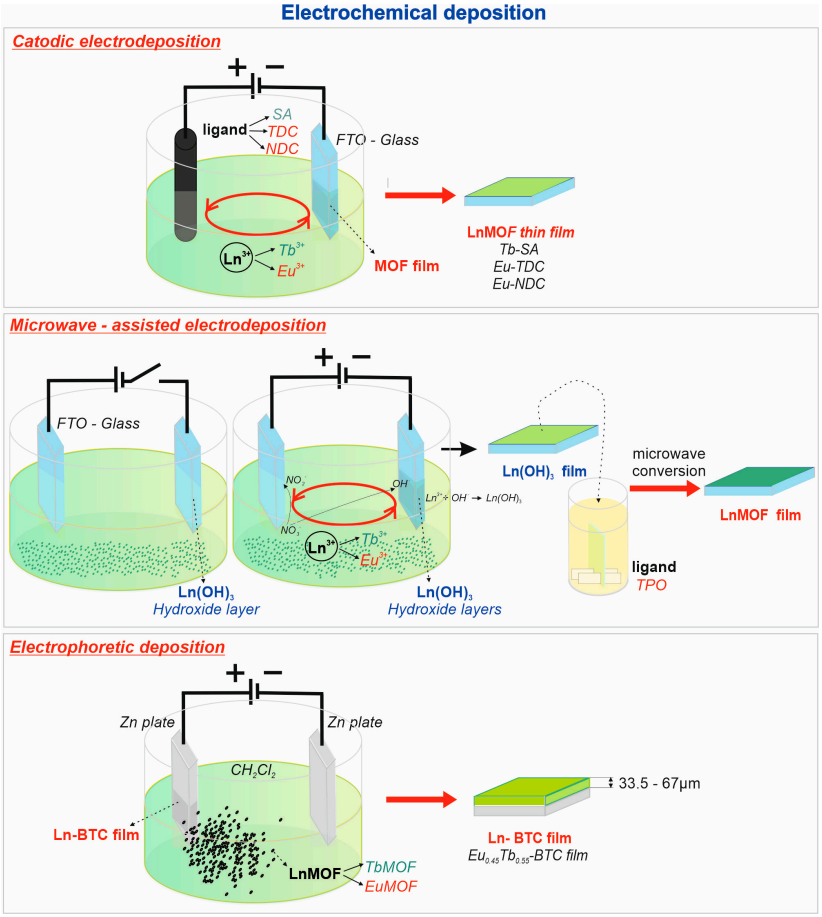

Figure 5. Schematic illustrations of electrochemical deposition of LnMOF films: cathodic electrodeposition of Eu-NDC, Eu-TDC, and Tb-SA films (separately) on FTO, adapted from [85–87]. Anodic electrodeposition of $Ln(OH)_3$ layers on FTO and their microwave conversion to Ln-BTC films (Ln = Eu, Tb), adapted from [88]. Electrophoretic deposition of $Eu_{0.45}Tb_{0.55}$-BTC film, adapted from [89].

2.3.1. Cathodic Electrodeposition

Electrochemical deposition, or simply ECD, includes cathodic (CED) [85–87], anodic (AED) [88] and electrophoretic (EPD) [89] depositions. It is a method that allows for the rapid fabrication of MOF-TFs with good electrical contact and mechanical adhesion between the deposited MOF-TF and the conductive substrate [90–92]. For cathodic deposition in Figure 5, both precursor ligands and metal ions are required to be present in the electrolyte, and the MOF thin film deposits on the surface of the cathode. For example, a pair of electrodes, a graphite rod as the anode and fluorine-doped tin oxide (FTO) conductive glass as the cathode, can be used for deposition of the nano-flake MOF—Eu-NDC TF [85] on the cathode from the blend of DMF, $Eu(NO_3)_3 \cdot 6H_2O$ and 2,6-naphthalene dicarboxylic acid during the galvanostatic electrolysis at a constant current. Similarly, this method has succeeded in the fabrication of an Eu-TDC film from a solution of $Eu(NO_3)_3$ and thiophene-2,5-dicarboxylic acid [86] and MOF terbium-succinate (Tb-SA) thin film [87], as shown in Figure 5, from the solution of $Tb(NO_3)_3$ and succinic acid in DMF, respectively. The XRD signals of Tb-SA film agree with the simulated XRD pattern of Holmium-SA [87]. The Eu-NDC, Eu-TDC, and Tb-SA films could be used as highly selective sensors for picric acid, nitrophenols, and Cu^{2+} ions, respectively. The other LnMOF films on the FTO substrate, e.g., Tb-BDC (sensor for Cu^{2+} ions) [93], Eu-HBPTC film (sensor for carbonate

ions; BPTC = benzophenone-3,3′,4,4′-tetracarboxylate) [94], and white-light-emitting Ln-HMA-TFs (Ln = Eu^{3+}, Gd^{3+}, Tb^{3+}; H_3HMA = hemimellitic acid) [95] were fabricated by the same approach.

2.3.2. Anodic Electrodeposition

In the case of anodic deposition (AED), the MOF-TFs are formed on the anodic site. Here the electrolyte contains only the precursor organic ligands. The metal ions required for the MOF construction originate from the anode itself [96,97]. A series of MOFs were prepared on the ITO glass metal through an anodic deposition. Zn-BTC film was grown on Zn-ITO in a mixed BTC and tetrabutylammonium tetrafluoroborate ($TBABF_4$) solution in water/ethanol [97]. Also, pure zinc as a counter-electrode was used. Also, Zn-PBDC film (BPDC = 4,4′-bipyridine, 2,2′-bipyridine-5,5′-dicarboxylic acid) can be prepared in a similar way [97].

While most of the MOF-TFs can be obtained utilizing metal or a metal-film electrode, it is still quite a challenge and a question of price to electrochemically deposit lanthanide metals as the electrodes for the fabrication of luminescent thin films. The team of Li et al. [88,98] developed a microwave-assisted electrochemical deposition technique for LnMOF-TFs (Figure 5). In their works, a dense and homogeneous $Ln(OH)_3$ (Ln = Eu, and Tb) layer was first formed on the FTO electrode after eight cycles of AED from the solution of $Ln(NO_3)_3$. Subsequently, the formed $Ln(OH)_3$ layer was converted to LnMOF-TFs by the use of microwave irradiation in a vessel containing the solution of TPO linker (TPO = tris-4-carboxylatephenyl phosphineoxide). It is also possible to combine the microwave-assisted ECD with lithography and obtain patterned LnMOF-TFs using this strategy by patterning poly(dimethylsiloxane) (PDMS) films on FTO glass. These patterned TFs have strong luminescence properties, which are of great interest in the fields of color displays, luminescent sensors structural probes, anticounterfeiting barcodes, prints, and watermarks [8,88].

2.3.3. Electrophoretic Deposition

The electrophoretic deposition (EPD) process is based on the surface charge of the MOF particles suspended in the liquid media. Thus, it is possible to deposit the MOF-TFs from colloidal MOF suspension onto one of the electrodes immersed in the solution/suspension. It can be achieved by applying a fixed voltage between electrodes, and driven by the electric field, the MOF particles will move toward the oppositely charged electrode and form a thin and mostly dense layer [99–101]. Figure 5 shows how LnMOFs-TFs of Tb-BTC, Eu-BTC, and $Eu_{0.45}Tb_{0.55}$-BTC were successfully and rapidly deposited on an unmodified substrate (zinc plate) in 5 min, achieving a thickness of about 33.5–67 µm. The XRD data of the Tb-BTC MOFs, are in agreement with the simulated $La(BTC)(H2O)_6$ [89]. The as-prepared Tb-BTC films exhibited exceptional sensitivity toward the detection of nitrobenzene and Cr^{3+} in solution along with trinitrotoluene and nitrobenzene in gaseous samples. Two types of dual-emitting Ln@UiO-66-Hybrid MOFs [102] with luminescent ligand and lanthanide metals integrated into a UiO-66-type structure and deposited on FTO by EPD were found to be suitable for ratiometric temperature-sensing [102]. The temperature range and relative sensitivity for Tb@UiO-66-Hybrid and Eu@UiO-66-Hybrid films were 303–353 and 303–403 K, along with 2.76 and 4.26% K^{-1}, respectively.

2.4. Ultrasonic Spray Deposition

As a member of an emerging group of strategies applied for MOF-TF fabrication and deposition, ultrasonic spray deposition should be mentioned [103–105]. Ultrasonic spray deposition, as a time-saving, low-cost, and new route for the fabrication of luminescent MOF films, can be considered an advancement in the integration of LnMOFs in future optical devices [5,48].

The schematic representation of the process is depicted in Figure 6. Here, two or more precursor solutions are used: (1) the source of metal ions and (2) the source of organic ligands. These solutions are atomized by separated ultrasonic nebulizers to form ultrafine

mists, which are further transferred by gas flow, mixed, and deposited onto the prepared substrate surface. This allows solvents to evaporate and MOFs to crystalize and form matrix-free TFs. This strategy allowed for the deposition of $Tb_2(BDC)_3$, where BDC = 1,4-benzenedicarboxylate, MOF-TFs on a variety of substrates, including glass, while retaining photoluminescent properties [48]. The temperature of the substrate plays a crucial role in the TFs formation process and thus impacts its final structure, morphology, and luminescent properties. It was found that low substrate temperatures resulted in the formation of films with higher luminescence intensities [48]. The XRD patterns of the $Tb_3(BDC)_3$ MOF films deposited onto a glass slide at different temperatures have a structure according to the respective JCPDS card (00-157-1127) [48]. The ultrasonic spray deposition approach proved itself as a cheap, promising, easily scalable, one and can be considered as a breakthrough for bringing MOFs to the commercial application in future optical devices.

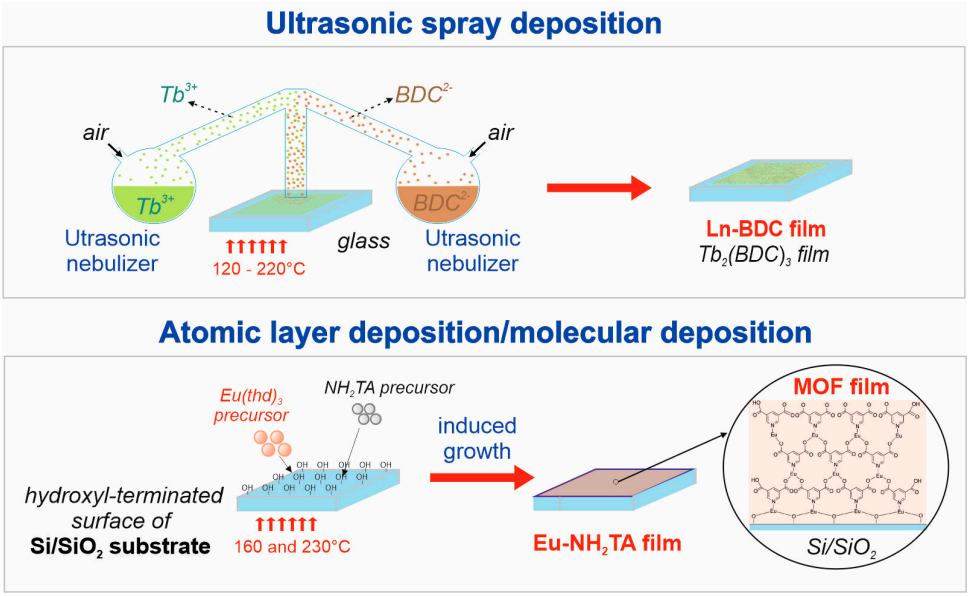

Figure 6. Scheme of the ultrasonic spray deposition equipment used for the preparation of Tb-BDC film on a glass slide with the adjustable process temperature from 120 to 220 °C. Adapted from [48]. Scheme of atomic layer deposition/molecular layer deposition for hybrid EuMOF film based on Eu-NH_2TA film. Figures Used were adapted from [106,107].

2.5. Atomic Layer Deposition/Molecular Layer Deposition

The Atomic Layer Deposition (ALD) technique is widely used in thin-film deposition due to its high precision and flexibility. As a state-of-the-art industrial thin-film deposition technique, it offers a simple way to control the film thickness at the atomic level and is available for the preparation of multilayer structures [8]. ALD equipment is expensive and the process is slow, which increases operating costs. Due to its small size, a microreactor can offer several advantages, including the rapid mixing of reactants. The use of a smaller volume of liquid enables a more ecological synthesis and reduces production costs.

It was used in seed-assisted secondary growth for MOF-TFs along with the metal precursor TFs. ALD can be directly employed to fabricate MOF-TFs via a vapor–solid reaction [8,106]. In a general fabrication process, the source of metal and organic precursors for the desired MOFs in the gaseous form are sequentially blown onto the surface of a substrate with a pulse of gas, where it reacts and forms the solid layer. Crystalline hybrid MOF-TFs of Eu-NH_2-TA, where TA = 2-aminoterephthalic acid (NH_2-TA), with a thickness of 22 µm were prepared by Atomic/Molecular Layer Deposition (ALD/MLD) on Si/SiO_2 substrate (Figure 6) [106,107]. Here, β-diketonate complex precursor europium(III)-tris-(2,2,6,6-tetramethyl-3,5-heptanedionate, $Eu(THD)_3$ reacted with NH_2-TA. The single-step synthesis proceeds without the need for a modulator. This procedure is a solvent-free green route, which does not require any post-synthesis treatment [107].

2.6. Composite Hybrid Films

The composite hybrid LnMOF-TFs were fabricated using modification by carbon dots (CDs) [67]; a variety of polymers, such as polyvinylidene difluoride PVDF [67,108]; ethyl cyanoacrylate (glue adhesive, marked as EVOB) [62]; polylactic acid [66]; polymethylmethacrylate (PMMA) [109,110]; along with a post-synthetic modification (PSM) with butyl methacrylate (BMA), which was initiated by benzoyl peroxide (BPO) [56]. Figure 7 depicts the various film preparation processes. Eu_xTb_{1-x}(L) and UiO-66(Zr&Eu) MOF films on glass were prepared using PMMA and PVDF, respectively, as a binder [108,110]. PMMA or PVDF were dissolved in DMF solution (for better dispersion of MOF powders).

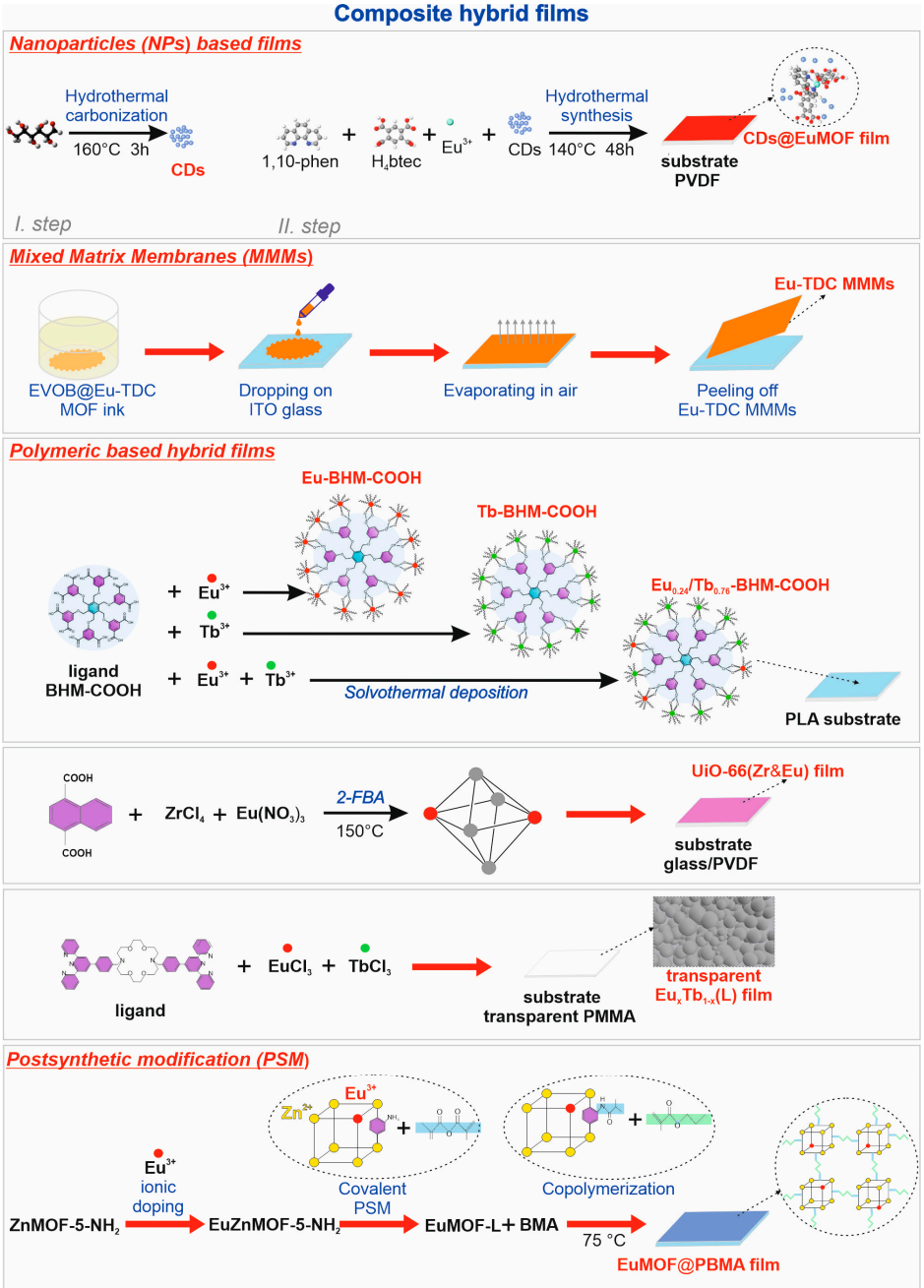

Figure 7. Schematic illustrations of preparation composite polymeric hybrid films (in descending order): CDs@Eu-MOF/PVDF TFs; Eu-TDC Mixed Matrix Membranes in EVOB membrane; polylactic acid (PLA)-based Ln-BHM-COOH-PLA films (Ln = Eu, Tb, $Eu_{0.24}Tb_{0.76}$); UiO-66(Zr&Eu)/PVDF films on the

glass; transparent Eu_xTb_{1-x}(L)@PMMA films; and post-synthetic modification (PSM) of Eu-MOF-L@PBMA film. Adapted from [56,62,66,67,108,110].

2.6.1. Nanoparticle-Based Films

Figure 7 shows the two-step synthesis process of novel fluorescent CDs@Eu-MOF/PVDF-TFs prepared by the simple combination of solvothermal synthesis and in-situ growth process [67]. First, a certain amount of carbon dots was solvothermally synthesized, then H_4btec = 1,2,4,5-benzenetetracarboxylic acid and 1,10-phen = 1,10-phenanthroline monohydrate were added and used as ligands—Eu^{3+} as the metal skeleton, and PVDF as the flexible substrate [67]. XRD reveals that the diffraction peaks of Eu-MOF and CDs@Eu-MOF are basically the same, indicating that the CDs have no impact on the crystal structure of Eu-MOF due to the small size of CDs and their embedding into the MOF [67]. CDs@Eu-MOFs/PVDF film can be used to detect nitrobenzene and 4-nitrophenol in both methanol solution and gaseous state.

2.6.2. Mixed Matrix Membranes

Luminescent mixed matrix membranes (MMMs) were synthesized by mixing ethyl cyanoacrylate solution, also known as 502 glue, by the brand EVO BOND (marked as EVOB) and micro-powder of Eu-TDC, where TDC is thiophene-2,5-dicarboxylate. The mixed slurry was then dropped on ITO glass and air-dried for 2 h to form luminescent MMMs (Figure 7). The XRD patterns of Eu-TDC MMMs contain the peaks of Eu-MOF and EVOB, indicating that the integrities of the MOF particles were well maintained during the preparation of the film [62]. The Eu-TDC MMM-based sensor can efficiently detect antibiotics of the nitroimidazole family (NIABs) in aqueous systems and provides excellent luminescent stability [62].

2.6.3. Polymeric-Based Hybrid Films

A series of luminescent Eu^{3+}/Tb^{3+}-MOFs were prepared using BHM-COOH—a novel ligand containing 12 carboxyl groups [66]. These MOFs can be used as a reliable bimetallic Ln-MOF luminescent sensing platform by simply combining a polylactic acid (PLA) layer as substrate with a $Eu_{0.24}Tb_{0.76}$-BHMCOOH film (Figure 7). This platform outperforms the traditional MOF-based ones applied for Fe^{3+} ions detection [66].

The novel smart thermometer based on dual-emitting solid film has been fabricated by mixing UiO-66(Zr&Eu) and PVDF. Here, UiO-66(Zr&Eu) was modified by replacing Zr^{4+} in clusters with Eu^{3+}, using 2-Fluorobenzoic acid (2-FBA) as a template (Figure 7) [108]. Similarly, a ratiometric luminescent thermometer was developed based on a transparent flexible film containing Eu^{3+}/Tb^{3+} lanthanide complexes in a PMMA-matrix, which was constructed via the solution casting method (Figure 7) [109,110]. The film with a 1:1 Eu^{3+}/Tb^{3+} molar ratio exhibits an excellent temperature-dependent behavior in the range of 77 to 297 K.

2.6.4. Postsynthetic Modification

Postsynthetic modification (PSM) was employed to improve the processing and application potentials of luminescent MOF-based hybrid polymeric films [56]. In particular, ZnMOF-5-NH_2 frameworks, as shown in Figure 7, were modified with Eu^{3+} to create red-emitting centers. Then, methacrylic anhydride was introduced, which reacted with amino groups of Eu-ZnMOF-5-NH_2, so Eu-MOF-L with unsaturated bonds was obtained by a PSM strategy. And finally, BPO-initiated copolymerization took place between Eu-MOF-L and butyl methacrylate (BMA). The resulting Eu-MOF-L@PBMA film is homogeneous, elastic, flexible [56], and has multiple luminescent centers. It can be applied both as a white-light-emitting material and as a sensor for VOC and amines.

2.7. Differences between Pure and Composite Films

LnMOF films have clear advantages over powder sensors, including portability, robust stability, and recyclability [72]. Single-Ln^{3+} LnMOFs exhibit basic luminescent phenomena, while mixed-Ln^{3+} LnMOFs demonstrate a significant capability for adjustable white light emission and temperature measurement [8]. Pure MOFs are promising sensing materials due to their extremely large surface area and porosity, which can enhance surface reactions with analytes [25]. The integration of MOF materials with high specific surface area, regular pore size, and adjustable structure with polymers is crucial for the creation of composite films with multiple applications [58]. The multi-color luminescence of Eu-MOF-L@PBMA polymeric hybrid films can be tuned by optimizing critical parameters to function as a white-light emitting device. Additionally, the film is used for the detection of volatile organic vapors [56].

MOFs come in various structures, such as nanocrystals, nanospheres, nanosheets, needles, thin films, membranes, and glasses [61]. Among these structures, LnMOF-TFs have garnered significant attention due to their immense potential in advancing nanotechnology applications in lighting, optical communications, photonics, and biomedical devices [61]. Porous nano-sized MOFs have certain advantages over traditional nanomaterials. The structural and compositional diversity allows for the fabrication of LnMOF films of different compositions, shapes, sizes, and physico-chemical properties [8].

3. Luminescent Properties of LnMOF-TFs

3.1. Structure of Ligands Involved in Coordination with Lanthanide Ions

The luminescent properties of lanthanide ions highly depend on the structural details of their coordination environment. The large variability of Ln ion–ligand combinations in MOFs enables multiple possible luminescence processes and has already led to a large number of luminescent materials. LnMOFs built using coordination bonds between Ln ions and organic ligands are hopeful materials due to their porous crystalline structures, rich mixtures, and simple preparation [71]. The availability of various building blocks of Ln ions and organic ligands allows access to fascinating structures, novel topologies, and the direct manipulation of their physical and chemical properties [8]. Organic linkers, through which lanthanide ions or nodes are connected, generally contain functional groups that are capable of forming coordination bonds, such as carboxylate, phosphate, sulfonate, amine, etc. [1].

The benzenetricarboxylate ligand is often used to prepare LnMOF films, e.g., Tb-BTC [71]. 1,3,5-benzenetricarbocylic acid (H_3BTC) possesses three carboxylic groups with multifarious coordination modes and could be regarded as a good candidate for an organic four-connected node [71]. The TbMOF (Tb-BTC) complex is a 3D open framework, and each asymmetric unit contains one eight-coordinated Tb^{3+} ion, one BTC ligand, two coordinated DMF molecules, and one free guest water molecule H_2O as $Tb(BTC)(DMF)_2.H_2O$ [71]. Each Tb^{3+} ion is coordinated with eight oxygen atoms from four BTC ligands through two chelating bidentate carboxylate groups, two monodentate carboxylate groups, and two terminal DMF molecules. The empirical formula is $C_{15}H_{19}N_2O_9Tb$ [71].

For the preparation of LnMOF films are commonly used ligands with the following structure: p-benzenedicarboxylate (BDC) [93]; BDC-NH_2 [73]; succinate (SA) [87]; bromomethylbenzene, dimethyl 5-hydroxy isophthalate (BHM-COOCH) [66]; benzophenone-3,3′,4,4′-tetracarboxylate (BPTC) [94]; 2,6-naphthalene dicarboxylate (NDC) [81]; thiophene-2,5-dicarboxylate (TDC) [86]; etc. The structure of BTEC and 1,10-PHEN as ligands, and Eu^{3+} as the metal skeleton [67], which adds a certain amount of carbon dots in novel composite film (CDs@Eu-MOF), are shown in Figure 7. A BHM-$COOCH_3$ ligand was synthesized for the preparation of Eu_xTb_{1-x}-BHM-COOH [66]. Additional structures of the ligands H_2NDC 2-FBA [108] and BDC-NH_2 [56] are observed in schematic illustrations.

Photoluminescent MOFs with the same lanthanide ion possess similar emission bands due to the state transitions characteristic for the particular cation: $^5D_0$ for Eu^{3+} and $^5D_4$ for Tb^{3+} [20,39,93]. Notably, different lanthanides can be combined in one MOF, thus

resulting in a combination of different emission spectra and luminous colors. The reported photoluminescence obtained in LnMOFs can be concluded as three types: lanthanide-centered luminescence, ligand-based, and guest-induced.

3.2. Lanthanide-Centered Luminescence

The luminescence of lanthanide ions originates from the energy transfer processes, also known in the literature as the "antenna effect" or "luminescence sensitization" (LS) [21]. The mechanism of LS within LnMOF-TFs is comprised of three steps: (1) light is absorbed by ligands around the lanthanide center; (2) energy is transferred to the lanthanide ions, and (3) luminescence is generated by the lanthanide ions (centers). White light-emitting $Tb_{10}Eu_1$-HMA LnMOF-TFs were fabricated via electrodeposition, and they show good photoluminescence with a satisfactory CIE coordinate of (0.33, 0.34) [95], which has been realized by electrodeposition for the first time. The average lifetime values achieved were 0.273 ms for Eu-HMA and 0.286 ms for Tb-HMA. The prepared new TFs show strong luminescence of Eu^{3+} and Tb^{3+} and are characterized by an efficient Tb^{3+}-to-Eu^{3+} energy transfer. Since then, a variety of MOF-TFs, such as EuMOF, TbMOF, and mixed LnMOF-TFs, have been reported [95].

3.3. Ligand-Based Luminescence

The Eu-BDC-NH_2 film was prepared by the new approach, namely the so-called "in situ secondary growth". It exhibits strong characteristic Eu^{3+} emission, which can be quenched by SO_2 gas [73]. The obtained Eu-BDC-NH_2 film has a wide range of potential applications, such as sensors, LEDs, solar cells, and TF transistors.

3.4. Guest-Induced Luminescence

Based on the large specific surface area and good absorption ability, MOFs often are used as a sorption platform; they can be used as a support or host for a variety of guest substances. Among the important ones will be the luminescent species, such as fluorescent quantum dots, dyes, and lanthanide ions/complexes. Very recently, fluorescent composites, such as CDs@Eu-MOF/PVDF and several materials from the QD@MOFs family, received great interest for their potential in chemical sensing, fluorescence imaging, and display lighting [67].

4. Light-Emitting Devices

The LnMOF thin films have a wide range of potential applications. Those of the most interest include sensors [111,112] and light-emitting devices (LEDs) [113]. Over the last decade materials science has focused on the development of solid-state white light (SSWL)-emitting materials, mainly thanks to their long operation lifetime and excellent efficiency [83]. These efforts resulted in the development of a new type of LnMOF-TFs—surface-supported MOFs, also known as Ln-SURMOFs. It can be fabricated LBL to combine several single light-emitting layers into composite solid-state white light-emitting devices [83]. For this reason, a deliberate design for SSWL performance was achieved by multiple emitting layers and the addition of three colors according to the RGB concept (red, green, and blue). The Tb/Eu/Gd-SURMOF RGB device shows CIE x,y coordinates close to ideal for white light (0.331, 0.329) excited by 360 nm (Figure 8) [83]. Prepared Ln-SURMOFs can be excited by different wavelengths (320 and 360 nm), and since the spectra exhibit excitation depending on maxima, this leads to a variation of the resulting chromaticity, as ascribed in Figure 8a. When observing the emission of a single Eu-SURMOF at 617 nm, the excitation spectrum displays a broadband shoulder at 250 nm, which is attributed to $\pi^*\leftarrow\pi/\pi^*\leftarrow$n ligand-based transitions [83]. Eu-SURMOF produces a magenta-colored emission that comprises both the ligand $\pi^*\rightarrow\pi/n^*\rightarrow\pi$ transitions and the typical Eu^{3+} $^5D_0\rightarrow{}^7F_J$ (J = 0–4) transitions, with $^5D_0\rightarrow{}^7F_2$ being the most intense and located at 617 nm. The high relative intensity of the ligand-based emission suggests an inefficient energy transfer process from the excited

states of the ligand to Eu^{3+} ions. The coordination polyhedron (LnO8) undergoes changes attributed to $\pi^*\leftarrow\pi/\pi^*\leftarrow$n ligand-based transitions.

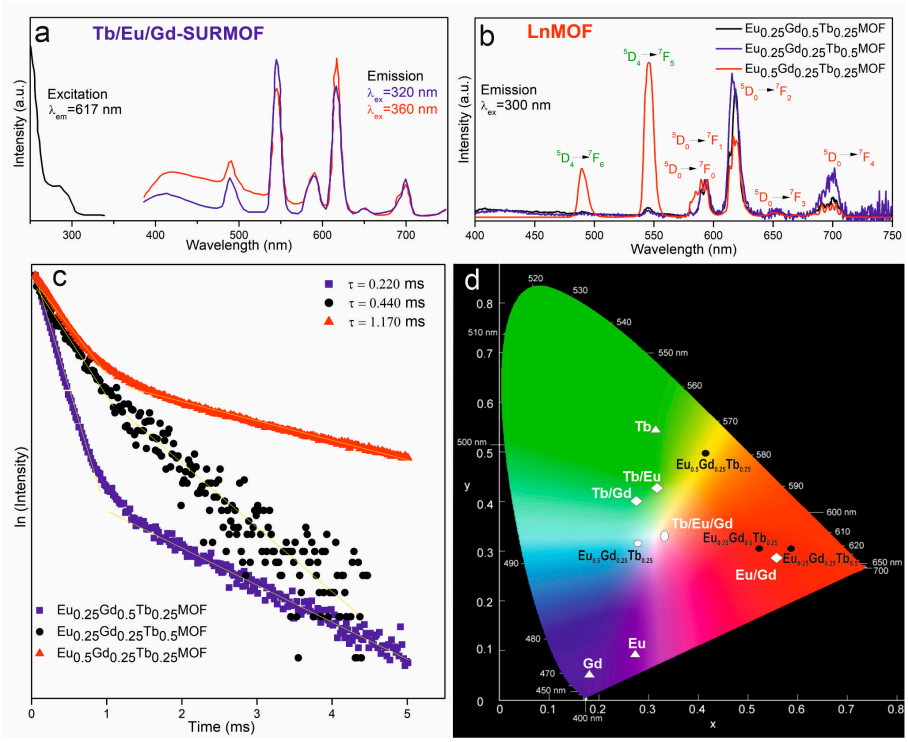

Figure 8. Comparison of Ln-SURMOF and LnMOF films: (**a**) excitation and emission spectra of white light-emitting Tb/Eu/Gd-SURMOF film; (**b**) emission spectra for three LnMOF films; (**c**) decay curves for LnMOF films; (**d**) illustration of CIE color diagram and chromaticity coordinates obtained for LnMOF (black) and Ln-SURMOF (white). Graphs are recreated based on data from [72,83].

Similar emission spectra were recorded for the Eu/Gd/TbMOF-TFs films prepared by the solvothermal method with three different concentrations of Eu, Gd, and Tb and are shown in Figure 8b. The spectra include the bands typical for Eu^{3+}, ascribed to transitions from the $^5D_0$ excited state to the ^7F_J (J = 0–4) ground states [72]. All films also exhibit bands at 486 and 542 nm characteristic for $^5D_4\rightarrow{}^7F_6$ and $^5D_4\rightarrow{}^7F_5$ transitions of Tb^{3+}, respectively. The decay curves for the Eu^{3+} ions for all films are shown in Figure 8c. The increase in the mol fraction of Eu in the film (from 0.25 up to 0.5) results in the improvement of the mean lifetime by more than five times and thus increases the quantum efficiency (η) (about 30.3%) compared to the similar Gd-based film (with a mol fraction of $Gd_{0.5}$). The mean lifetime values for the samples $Gd_{0.5}$-, $Tb_{0.5}$-, and $Eu_{0.5}$-based films were 0.220, 0.440, and 1.170 ms for Eu^{3+} emission ($^5D_0\rightarrow{}^7F_2$ transition) and 0.210, 0.220 and 0.530 ms for Tb^{3+} emission ($^5D_4\rightarrow{}^7F_6$ transition), respectively.

The CIE chromaticity coordinates for different Eu/Tb/Gd-SURMOF and LnMOF films fabricated both by LBL and solvothermal deposition are gathered in Figure 8d for comparison. When excited by 300 nm light, the films with a fraction of $Gd_{0.5}$ and $Tb_{0.5}$ refers to CIE coordinates in the red region due to the higher intensity of europium emission bands. When the excitation wavelength was changed to 394 nm, those CIE coordinates were (0.280, 0.310). Tb^{3+}- and Eu^{3+}-centered transitions were observed and dominated in the single- and double-layer Tb/Eu-SURMOFs. In the triple-layer setting, both hypersensitive transitions exhibit higher intensities in comparison to the double- and single-layered Ln-SURMOFs, which is a condition to yield white light emission in MOF systems [84]. Upon excitation at 360 nm [83], the emission spectrum of the triple layer Tb/Eu/Gd-SURMOF (Figure 8a) exhibits almost ideal white light emission, showing CIE x,y coordinates of (0.331, 0.329) corresponding to the center of the CIE diagram (see Figure 9d) and representing a real

RGB-SURMOF architecture. The corresponding values for a perfect white light emitter are (0.333, 0.333). The values of determined luminescence parameters of LnMOF films prepared by various methods are presented in Table 1.

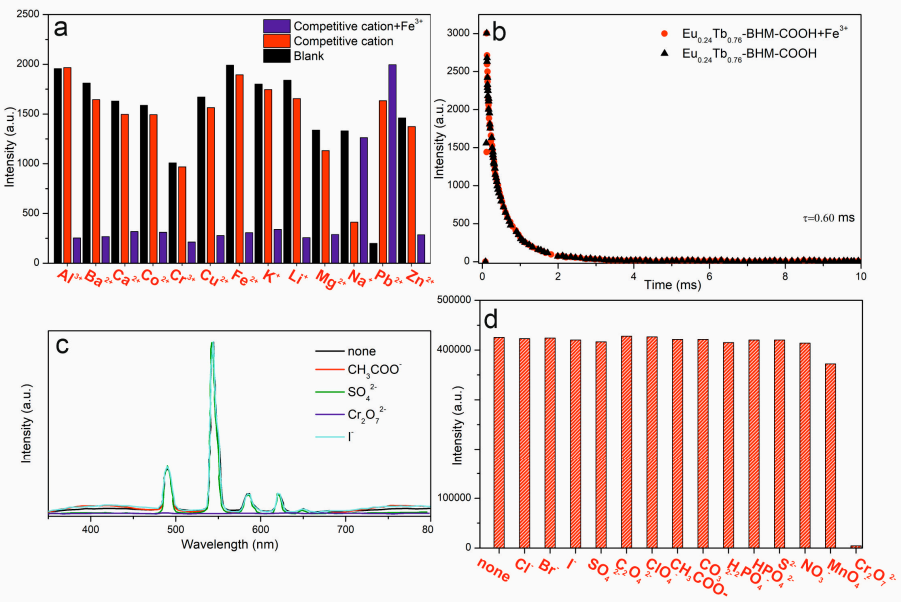

Figure 9. (**a**) Luminescence intensity of $Eu_{0.24}Tb_{0.76}$-BHM-COOH-PLA film (λ_{ex}: 314 nm): blank (black column), another single metal ion (red column), and add Fe^{3+} (purple column). (**b**) Decay curve of film in presence or absence of Fe^{3+} ions [66]. (**c**) Emission spectra of Tb-CPON-PMMA film toward different anions. (**d**) Comparison of luminescence intensities of $^5D_4 \rightarrow {}^7F_5$ transition at 545 nm for film in different anions [114]. Graphs are recreated based on data from [66,114].

Table 1. Luminescent properties of white light-emitting LnMOF thin films.

Eu/Gd/Tb/MOF	Deposition Method	Used Substrate	CIE Coordinates (x; y)	$Eu^{3+} \rightarrow$ τ (ms)	$Tb^{3+} \rightarrow$ τ (ms)	η (%)	Ref.
Tb-HMA	ECD	FTO	-	-	0.286	38.42	[95]
Eu-HMA	ECD	FTO	-	0.273	-	4.66	[95]
$Tb_{10}Eu_1$-HMA	ECD	FTO	0.330; 0.340	-	0.735	11.41	[95]
$Tb_{10}Gd_1$-HMA	ECD	FTO	-	-	0.449	47.79	[95]
Eu-MOF-L@PBMA	PSM	glass	0.293; 0.299	-	-	-	[56]
Tb/Eu/Gd-BTC SURMOF	LBL	quartz	0.331; 0.329	-	-	-	[83]
$Eu_{0.25}Gd_{0.5}Tb_{0.25}$-BTC	HT green	$Pt/SiO_2/Si$	0.520; 0.300	0.220	0.210	7.7	[72]
$Eu_{0.25}Gd_{0.25}Tb_{0.5}$-BTC	HT green	$Pt/SiO_2/Si$	0.590; 0.300	0.440	0.220	21.5	[72]
$Eu_{0.5}Gd_{0.25}Tb_{0.25}$-BTC	HT green	$Pt/SiO_2/Si$	0.280; 0.310	1.170	0.530	30.3	[72]

Eu-HMA, Tb-HMA, $Tb_{10}Eu_1$-HMA, and $Tb_{10}Gd_1$-HMA films realized by electrodeposition [95] provide an effective platform for energy transfer between the lanthanide ions due to the short intermetallic distances. $Tb_{10}Eu_1$-HMA film shows good photoluminescence with satisfactory CIE coordinates of (0.33, 0.34). When the polymeric hybrid of Eu-MOF-L@PBMA-TFs are excited at 335 nm, the emission coordinates situate at (0.2929, 0.2985), which corresponds to the almost ideal white light chromaticity at (0.330, 0.330) [56].

5. Application of LnMOF Films as Sensors

LnMOFs have been widely studied in various sensor applications due to their high porosity, surface area, and the particular luminescence of Ln^{3+} ions. Most of the LnMOF-based sensors show luminescence intensity changes, including luminescence enhancement–turn-on response and quenching–turn-off response, as a detected signal for the analytes

recognition. Eu^{3+} and Tb^{3+} are commonly used as luminescent centers in LnMOF sensors because of their strong red emission at ~614 nm and green emission at ~541 nm, respectively [20,115]. Synthetic innovations enabling the development of MOF thin films have produced a range of sensing technologies capable of the selective detection of a variety of analytes, including ions, small molecules, gases, temperature, and biological analytes of interest using optical, electrical, and acoustic techniques [3]. Recently reported luminescent LnMOFs films as sensors fabricated by various methods are listed in Table 2.

Table 2. Applications of LnMOF thin films as luminescent sensors.

LnMOF Film	Growth/Coating Method	Substrate	Target Analyte	Film Thickness (μm)	Ref.
Eu-BQDC	ST/ECD	ITO	Hg^{2+}	10	[116]
Tb-BDC	ECD	FTO	Cu^{2+}	2	[93]
Tb-SA	ST/ECD	FTO	Cu^{2+}	1	[87]
Tb-BTC	LBL	Silk fiber	Cu^{2+}	10	[82]
Tb-BTC	ST/EPD	Zn plate	Cr^{3+}, NB; TNT	55	[89]
$Eu_{0.24}Tb_{0.76}$-BHM-COOH-PLA	ST/drop-cast	glass	Fe^{3+}	-	[66]
Eu-HBPTC	ST/ECD	FTO	CO_3^{2-}	-	[94]
Tb-CPON-PMMA	ST/SC	glass	$Cr_2O_7^{2-}$	-	[114]
Tb-BTC	ST/DC	ITO	Organic solvents	7	[69]
Eu-NDC@HPAN	HT/LBL	HPAN	Formaldehyde	2–4	[81]
Eu-BDC-NH_2	ST	glass	Gaseous SO_2	1	[73]
Eu@UMOF-LA	PSM	Al_2O_3	NH_3	50	[117]
Eu-MOF-L@PBMA	PSM	glass	Organic vapors	-	[56]
Tb-BTC	ECD	Al	DNT	-	[118]
Eu-TDC	ECD	FTO	Nitrophenols	7	[86]
Eu-NDC	ECD	FTO	PA, TNP	0.05	[85]
CDs@Eu-PHEN-BTEC/PVDF	ST	PVDF	NB, 4-NP	-	[67]
$Gd_{0.9}Tb_{0.1}$HL	ST	Gd_2O_3	Ratiom. thermometer	10	[46]
UiO-66(Zr&Eu)/PVDF	HT;/DC	glass	Smart thermometer	30	[108]
$Eu_{0.5}Tb_{0.5}$(L)1@PMMA	ST	glass	Ratiom. thermometer	-	[110]
$Eu_{0.1}Tb_{0.9}$-BTC	ST/DC	ITO	Pharmaceuticals	4	[40]
Eu-TDC MMMs	ST	ITO	Pharmaceuticals NIABs	-	[62]
$Eu_{0.047}Tb_{0.953}H_2$L@PVDF	ST/SC	glass	COVID-19 Favipiravir	-	[119]

5.1. Cations Sensing

Detecting the metal ions with high precision and sensitivity is of great significance in environmental and biological studies, especially transition metal cations, such as Zn^{2+}, Cu^{2+}, Fe^{3+}, and Fe^{2+}, which are essential for a healthy metabolism. A highly luminescent Eu-BQDC film (BQDC = 2,2-biquinoline-4,4-dicarboxylate) was prepared by electrodeposition in combination with subsequent solvothermal synthesis. It exhibits high sensitivity and selectivity toward Hg^{2+} [116]. While similarly prepared on FTO substrates, Tb-BDC [93] and Tb-SA [87] TFs are selective toward Cu^{2+} in DMF solutions. The lifetime of Tb-BDC film and Tb-BDC + Cu^{2+} were 1.023 and 0.934 ms, respectively. Photoluminescent measurements demonstrated that Tb-SA films were relatively water-stable and had a fast response to Cu^{2+} ion aqueous media. The lifetime of Tb-SA + Cu^{2+} (1.088 ms) was decreased compared to Tb-SA (1.148 ms). The new Tb-BTC composite (MOF-76@silk fiber) was developed LBL for utilization in the colorimetric and fluorescent detection of aquatic Cu^{2+} with a detection limit down to 0.5 mg/L [82]. The quenching effect of this composite in the condition of Cu^{2+} was first reported with a very high selectivity and sensitivity. Luminescent Tb-BTC film prepared by EPD on the zinc plate was successfully used for the detection of Cr^{3+} ions in a water solution [89].

$Eu_{0.24}Tb_{0.76}$-BHM-COOH-PLA TFs were successfully applied as sensors for Fe^{3+} [66]. To study the selectivity of the LnMOF-TFs toward Fe^{3+}, sensing experiments with introduced interferents—one or more other metal ions—were carried out. As shown in Figure 9a, the sensitivity of $Eu_{0.24}Tb_{0.76}$-BHM-COOH-PLA LnMOF-TF toward Fe^{3+} (quenching performance) is not influenced by the presence of other cations. It confirms the potential of the mentioned LnMOF-TF for application as a highly selective luminescent sensor for Fe^{3+} in an aqueous media. Also, the concentration-dependent lifetime test was conducted to investigate the mechanism of quenching: as a result, the lifetime of the film (τ = 0.60 ms) in the aqueous system does not change with the increasing of Fe^{3+} concentration (Figure 9b). This ruled out the cause of dynamic quenching, indicating that the fluorescence quenching process is static quenching.

5.2. Anions Sensing

The Tb-CPON-PMMA polymer composite film, where CPON = 5-(4-carboxy-phenoxy)-nicotinic acid, composed of Tb-CPON and PMMA exhibits superior luminescent properties compared to pure LnMOF [114]. The Tb-CPON-PMMA film exhibits an excellent sensitivity toward $Cr_2O_7^{2-}$, with a high selectivity and detection limit of 5.6 ppb, which is much lower than the maximum contamination standard of 100 ppb in drinking water. The calculated luminescence lifetime of Tb-CPON was 1.032 ms, and the overall quantum yield was determined to be 62.7%. Figures 9c and 9d show the luminescence emission spectra and relative intensities of the prepared films in the presence of different anions, respectively. The sensitivity of the Tb-CPON-PMMA toward $Cr_2O_7^{2-}$ manifests itself in the quenching effect.

Another luminescent Eu-HBPTC thin film, where BPTC = benzophenone-3,3′,4,4′-tetracarboxylate, was successfully fabricated by EPD in an anhydride system and is highly selective toward carbonate ions in aqueous media [94].

5.3. Small Molecules, Gas, and Vapor Sensing

Sensing based on measuring the luminescent properties has proven to be an excellent detection technique for a variety of chemical substances, including gases and nitroaromatics thanks to its speed and cost-effectiveness. The nanosized Tb-BTC LnMOF-TFs prepared by dip-coating on ITO glass exhibited the highly sensitive and selective detection of organic solvents [69]. Eu-NDC@HPAN deposited on HPAN by the LBL method was used as a self-calibrating luminescent sensor for detecting small molecules, such as formaldehyde, in an aqueous media [81]. The Eu-BDC-NH_2 TFs on glass exhibit strong characteristic Eu^{3+} emissions, which can be fast and remarkably quenched by the presence of SO_2 [73]. The limit of detection (LOD) for SO_2 is calculated to be 0.65 ppm at a response time of 6 s. Transparent Eu@UMOF-Eu-LA film fabricated by the PSM method can selectively recognize and detect NH_3 in indoor polluted air with a detection limit of 9 ppm, which is lower than the minimum injuring concentration of 35 ppm [117]. Polymeric hybrid Eu-MOF-L@PBMA TF functionalized by versatile post-synthetic modification was utilized for the detection of volatile organic vapors, especially organic amines [56]. The luminescent films prepared by electrochemical deposition showed potential toward the detection of nitroaromatic explosives; Tb-BTC on an Al plate has been successfully tested for the detection of 2,4-dinitrotoluene (DNT) [118]. The luminescence lifetime of the sample changed from 0.48 ms to 0.58 ms when the layer was exposed to DNT vapors. Eu-TDC on FTO was used for nitrophenols and nitrobenzene detection in the vapor state [86]. The luminescence signal of Eu-NDC on an FTO film was strongly quenched by picric acid traces with good selectivity over other nitroaromatic explosives [85].

CDs@Eu-MOF/PVDF thin film was prepared using 1,2,4,5-benzenetetracarboxylic acid (H_4BTEC) and 1,10-phenanthroline monohydrate (1,10-PHEN) as ligands by the solvothermal method and modified by carbon quantum dots (CDs) by in-situ growth. The CDs@Eu-MOF composite film has strong red fluorescence along with good stability in methanol and shows high selectivity and sensitivity to nitrobenzene (NB) and 4-nitrophenol

(4-NP) [67]. The CDs@Eu-MOF/PVDF film can be used to detect nitrobenzene and 4-nitrophenol in both methanol solvent and gaseous state. The LOD for nitrobenzene and 4-nitrophenol in liquid are 0.2807 mg/L and 0.0168 mg/L, respectively, while in gaseous form, it is 0.346 mg/L and 0.0136 mg/L, respectively. Figure 10a shows that the selectivity exhibited by the film is consistent with the selectivity result of the powder. This indicates that CDs@Eu-MOF-PVDF film can be used to detect NB and 4-NP. The material retains a good luminescence signal measured in MeOH. The luminescence spectra of CDs@Eu-MOF/PVDF film in different concentrations of NB in MeOH were measured and presented in Figure 10b.

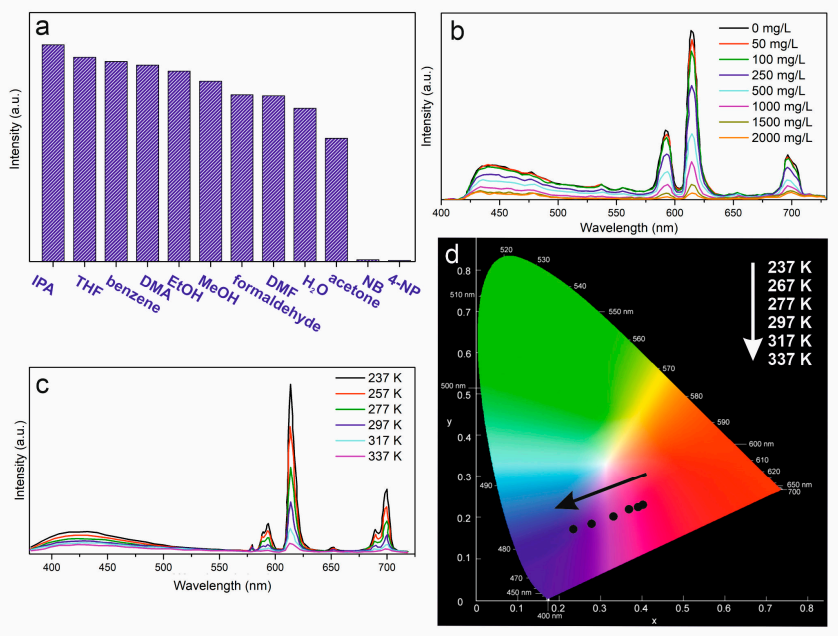

Figure 10. (**a**) Intensities of the luminescence of CDs@Eu-MOF/PVDF film immersed in different organic solvents and (**b**) fluorescence response of film in different concentrations of nitrobenzene (NB) solution [67]. (**c**) Temperature-dependent emission spectra (λ_{ex} = 360 nm) of UiO-66(Zr&Eu)/PVDF film conducted in the temperature range from 237 to 337 K and (**d**) the corresponding CIE picture of film at a different temperature [108]. Graphs are recreated based on data from [67,108].

5.4. Temperature Sensing

Luminescence-based sensors for temperature determination have achieved great attention based on their advantages, which include noninvasiveness, high accuracy, and spatial resolution—and (maybe) the most important, the ability to work in strong electro or magnetic fields [20], which makes impossible to use electronics for these purposes. The prepared polymer-MOF hybrid membranes show good temperature-sensing behavior. The maximal intensity ratio of the $^5D_4 \rightarrow {}^7F_5$ (Tb^{3+}) to $^5D_0 \rightarrow {}^7F_2$ (Eu^{3+}) transitions can be linearly related to the temperature in the range from 90 up to 240 K [120]. UiO-66(Zr&Eu)/PVDF can be used as a smart thermometer for the detection of temperature change in the temperature range from 237 to 337 K [108]. The relative sensitivity of the film is 4.26% K^{-1} at 337 K, which is the highest reported to date for MOF materials at this temperature. It can be explained by the unique energy transfer between the ligand and Eu^{3+} in the clusters. The temperature-dependent photoluminescence spectra of UiO-66(Zr&Eu)/PVDF were recorded in the range from 237 K to 337 K under excitation of 360 nm and are depicted in Figure 10c. The film showed satisfying temperature sensing characteristics. In addition, when changing the temperature from 237 K to 337 K, the films exhibited a shift from pink emission to blue emission, which suggested that the temperature variation could be distinguished also via the naked eye (Figure 10d).

The $Gd_{0.9}Tb_{0.1}HL$ film on Gd_2O_3 can be used as a thermometer in the range from 110 to 250 K, and a relative sensitivity up to 0.8% K^{-1}, whereas the compound $Gd_{0.99}Tb_{0.01}HL$ with a lower Tb content resulted in a relative sensitivity up to 4.4% K^{-1} at 110 K [46]. Transparent $Eu_{0.5}Tb_{0.5}$(L)1@PMMA film consisting of Eu^{3+}/Tb^{3+} lanthanide complexes and polymer PMMA exhibits a brilliant temperature-dependent luminescent behavior from 77 K to 297 K, enabling it to be a candidate for new ratiometric luminescent thermometers [110]. The combined Eu^{3+}/Tb^{3+}-based thermometer displays higher photo and thermostability compared to the pure complexes.

5.5. Sensing of Biomolecules

In recent years, the analysis of various pharmaceuticals, drugs, their derivates, and further metabolites has become a thing of high priority due to their both actual and possible long-term impact on biological/environmental systems [40,62,119,121–125]. Optical sensing has been considered a promising technique as it could offer sensitive, facile, and fast assays. Wang et al. [119] reported the first ratiometric luminescent sensor based on a new water-stable LnMOF polymer thin film ($Eu_{0.047}Tb_{0.953}$MOF@PVDF) prepared by a combination of solvothermal synthesis and spin-coating on the glass substrate, offering high sensitivity and selective detection towards the potential COVID-19 drug favipiravir. The associated MOF drug quenching effect is found to be selective towards other potential COVID-19 drugs.

The Eu-TDC-based MMMs as a sensor can efficiently detect nitroimidazole and other antibiotics from the same family, such as dimetridazole and metronidazole (NIABs), in an aqueous system due to its excellent luminescent stability [62]. The Eu-TDC MMMs have the advantages both of polymers and MOFs, which provide high flexibility and extend their applicability. The Eu-TDC MMMs are not affected by other antibiotics or ions when detecting NIABs in water solutions and show lower LODs (0.58 mg/L for metronidazole and 0.51 mg/L for dimetridazole) with a wider linear range. The mechanism operating in NIAB-sensing is considered to be a strong inner filter effect between the Eu-TDC MMMs and NIABs. The overlaps between the absorption spectra of antibiotics and the excitation spectrum of Eu-TDC MMMs are shown in Figure 11a. We can see that NIABs (320 nm) have greater spectral overlaps with Eu-TDC MMMs (324 nm) than other antibiotics.

The LnMOF-TF compound was synthesized using a solvothermal method and subsequently employed to fabricate the mixed-crystal $Eu_{0.1}Tb_{0.9}$-BTC TF by dip-coating it on an ITO substrate [40]. The film's luminescence varies depending on the guest molecules, making it an excellent candidate for self-referencing and self-calibrating luminescent sensors. This is achieved by establishing a fingerprint correlation between each pharmaceutical molecule and the corresponding change in emission intensity. The intensity ratio exhibits a linear relationship with the pharmaceutical concentration within a certain range. The $Eu_{0.1}Tb_{0.9}$-BTC film emits light of different colors, which are in good agreement with the calculated chromaticity coordinates on the basis of the CIE chromaticity diagram (Figure 11b).

Compared to the most luminescent MOF sensors based on powders, films can be easily reused after washing with the proper solvent. The Eu-TDC MMMs are expected to have recycling properties due to their stability in aqueous media [62]. The reproducibility of Eu-TDC MMMs was determined by recording the fluorescence intensity of the film in an aqueous solution of 0.2 mM dimetridazole and blank solution after it was washed with tap water. As shown in Figure 11c, the MMM sensor exhibits an "ON/OFF-ON" switching pattern with almost no change in the fluorescence intensity of the Eu-TDC MMMs after being repeated five times, indicating that Eu-TDC MMMs have excellent reusability. The used Tb-CPON-PMMA strips [117] were washed with distilled water several times, and then the corresponding luminescence intensities were recorded (Figure 11d). The recorded relative intensities after five cycles showed the luminescence intensity could be maintained after five detection/washing cycles. These results indicate that the Tb-CPON-PMMA-based

sensor may be one of the new generations of sustainable test assays for dichromate ions detection, even on-site "in the field".

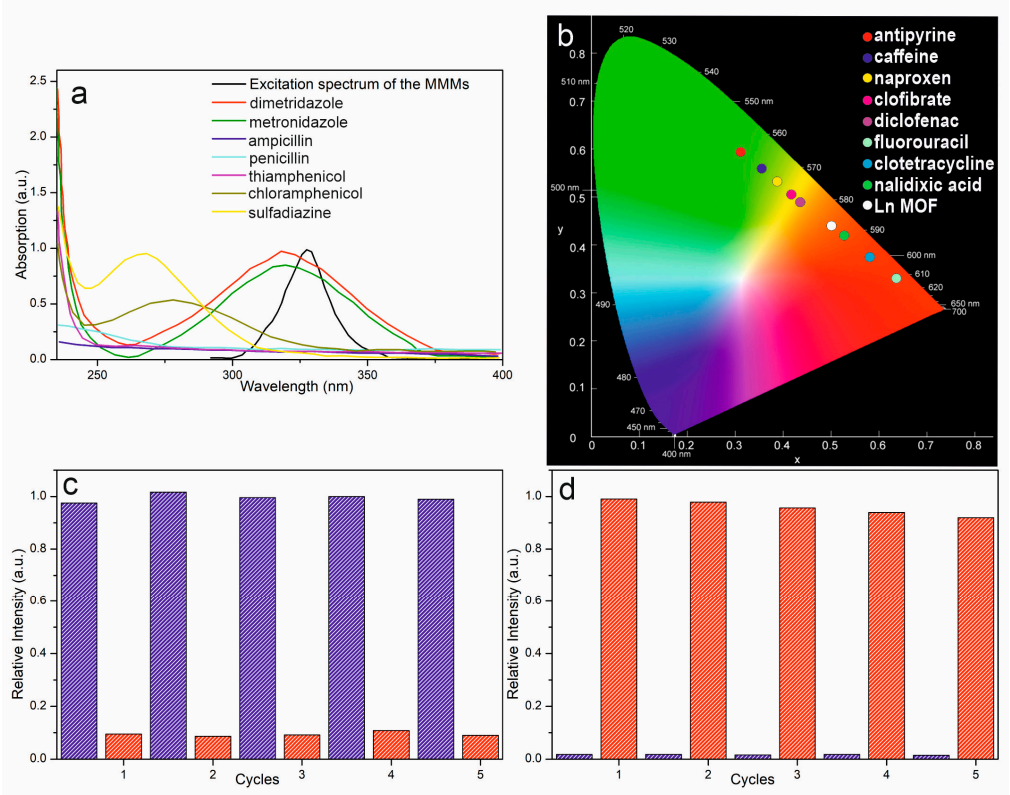

Figure 11. (**a**) UV-vis absorption spectra of different nitroimidazole antibiotics and excitation spectrum of Eu-TDC MMMs [62]. (**b**) CIE chromaticity coordinates of $Eu_{0.1}Tb_{0.9}$-BTC thin film in the presence of different pharmaceutical analytes [40]. (**c**) Reusability of the Eu-TDC MMMs toward the detection of metronidazole in aqueous media [62]. (**d**) Relative intensities for composite Tb-CPON-PMMA film reused for several cycles [114]. Graphs are recreated based on data obtained from [40,62,114].

The fluorescence signal of the Eu-TDC thin film can be recovered by washing it with methanol, which restores the fluorescence intensity to its original state [86]. The rinsed film can then be reused to detect nitrophenol TNP. The results indicate that the fluorescence intensity and quenching ability of the Eu-TDC thin film remain largely unchanged even after five cycles of use. Similarly, the UiO-66(Zr&Eu)/PVDF film thermometer [108] exhibits a stable optical characteristic, as evidenced by the unaltered intensity ratio when subjected to temperature cycles ranging from 237 K to 337 K. Furthermore, the temperature sensing performance of the polymer films surpasses that of the powders, and the sensor can be reused up to three times without any loss in performance.

6. Conclusions and Future Outlook

This review summarizes the recent progress in luminescent LnMOF-TFs based on Eu, Tb, and Gd from the point of view of preparation techniques and modification methods, along with applications in sensors and light-emitting devices. Many reviews already mapped the preparation of LnMOF films but only as a subclass of other MOF films. Covered here are recent technologies based on LnMOF-TFs that have the potential to significantly benefit energy, manufacturing, and environmental sectors.

The preparation of highly oriented single-crystal and polycrystalline LnMOF-TFs poses a significant challenge. The methods employed to assemble luminescent LnMOF-TFs form the basis of these challenges. Despite the potential benefits, the commercialization of MOF films is expected to be difficult in the near future due to the requirements for cost-

effective scale-up production. Currently, there is no perfect technique that can satisfy all the requirements for commercialization. Most of the reported methods for fabricating LnMOF thin films are only applicable to specific MOFs under laboratory conditions. Therefore, it is crucial to explore more facile and flexible methods for LnMOF thin film fabrication. Direct synthesis and secondary growth strategies based on traditional hydro/solvothermal synthesis remain the most widely used methods. However, other techniques, such as LBL deposition, ECD, EPD, DC deposition, and SC deposition, are prevalent in the manufacturing of LnMOF films. LBL deposition enables the fabrication of various film types, offering excellent control over film thickness and enabling the creation of complex MOF heterostructures. The ECD method allows for the rapid fabrication of defect-free films with controllable thicknesses. The ALD technique provides an easy way to control film thickness at an atomic level and is suitable for fabricating multilayer structures.

Recent advancements in continuous flow microreactors and process automation have opened up new opportunities for advancing progress in LnMOF synthesis. The use of less liquid volume allows for greener synthesis, reducing production costs. Current progress in using automatic methods for LnMOF synthesis has demonstrated promising results in the preparation of composite hybrid films.

Luminescent LnMOF-TFs have received great attention in a wider range of applications, both as light-emitting devices and sensors. The LnMOFs based on Eu, Tb, and Gd, their combinations, and different ligands have been reported, making it possible to integrate these MOFs into practical and useful devices. Lanthanide complexes and LnMOF films have efficacious utility as prospective white light-emitting materials. Ln-based LEDs with excellent color purity have become increasingly common.

This review also covers the recent research progress on luminescent LnMOF films and their applications in sensing cations, anions, small molecules, nitroaromatic explosives, gases, vapors, temperature, and biomolecules. The sensing functionality of LnMOF films is based on their luminescence changes in response to different analytes. However, the sensing performances are significantly influenced by the film thickness.

This review summarized and analyzed existing manufacturing technique progress in recent years for luminescent LnMOF films and their applications as light-emitting devices and sensors. It is believed that these advances will definitely extend the applications of LnMOFs to optoelectronic devices and are likely to create impactful innovation in the field of LnMOF films.

Author Contributions: Investigation, conceptualization, resources, methodology, writing—original draft preparation, H.B.; writing—review and editing, visualization, data curation, formal analysis, H.B., E.M. and I.S. All authors have read and agreed to the published version of the manuscript.

Funding: This research was funded by the Grant Agency of the Slovak Academy of Sciences through project VEGA No. 2/0027/23 and APVV-20-0299.

Data Availability Statement: The data presented in this study are available upon request from the corresponding author.

Conflicts of Interest: The authors declare no conflict of interest. The funders had no role in the design of the study, interpretation of data, or the writing of the manuscript.

References

1. Chen, F.; Drake, H.F.; Feng, L.; Powell, J.A.; Wang, K.Y.; Yan, T.H.; Zhou, H.C. Metal–Organic Frameworks as Versatile Platforms for Organometallic Chemistry. *Inorganics* **2021**, *9*, 27. [CrossRef]
2. Gangu, K.K.; Maddila, S.; Jonnalagadda, S.B. The Pioneering Role of Metal-Organic Framework-5 in Ever-Growing Contemporary Applications—A Review. *RSC Adv.* **2022**, *12*, 14282–14298. [CrossRef]
3. Ellis, J.E.; Crawford, S.E.; Kim, K.J. Metal-Organic Framework Thin Films as Versatile Chemical Sensing Materials. *Mater. Adv.* **2021**, *2*, 6169–6196. [CrossRef]
4. Song, X.Z.; Song, S.Y.; Zhang, H.J. Luminescent Lanthanide Metal-Organic Frameworks. *Struct. Bond.* **2015**, *163*, 109–144. [CrossRef]

5. Zhuang, Z.; Liu, D. *Conductive MOFs with Photophysical Properties: Applications and Thin-Film Fabrication*; Springer: Singapore, 2020; Volume 12, ISBN 0123456789.
6. Bai, W.; Li, S.; Ma, J.; Cao, W.; Zheng, J. Ultrathin 2D Metal-Organic Framework (Nanosheets and Nanofilms)-Based: X D-2D Hybrid Nanostructures as Biomimetic Enzymes and Supercapacitors. *J. Mater. Chem. A* **2019**, *7*, 9086–9098. [CrossRef]
7. Xu, G.; Yamada, T.; Otsubo, K.; Sakaida, S.; Kitagawa, H. Facile "Modular Assembly" for Fast Construction of a Highly Oriented Crystalline MOF Nanofilm. *J. Am. Chem. Soc.* **2012**, *134*, 16524–16527. [CrossRef]
8. Zhang, Y.; Chang, C.H. Metal-Organic Framework Thin Films: Fabrication, Modification, and Patterning. *Processes* **2020**, *8*, 377. [CrossRef]
9. Soni, S.; Bajpai, P.K.; Arora, C. A Review on Metal-Organic Framework: Synthesis, Properties and Application. *Charact. Appl. Nanomater.* **2020**, *3*, 551. [CrossRef]
10. Meyer, L.V.; Schönfeld, F.; Buschbaum, K.M. Lanthanide Based Tuning of Luminescence in MOFs and Dense Frameworks—From Mono- and Multimetal Systems to Sensors and Films. *Chem. Commun.* **2014**, *50*, 8093–8108. [CrossRef]
11. Liu, W.; Huang, X.; Chen, C.; Xu, C.; Ma, J.; Yang, L.; Wang, W.; Dou, W.; Liu, W. Function-Oriented: The Construction of Lanthanide MOF Luminescent Sensors Containing Dual-Function Urea Hydrogen-Bond Sites for Efficient Detection of Picric Acid. *Chem. A Eur. J.* **2019**, *25*, 1090–1097. [CrossRef]
12. Li, Y.-Z.; Fu, Z.-H.; Xu, G. Metal-Organic Framework Nanosheets: Preparation and Applications. *Coord. Chem. Rev.* **2019**, *388*, 79–106. [CrossRef]
13. Luo, J.; Li, Y.; Zhang, H.; Wang, A.; Lo, W.S.; Dong, Q.; Wong, N.; Povinelli, C.; Shao, Y.; Chereddy, S.; et al. A Metal–Organic Framework Thin Film for Selective Mg^{2+} Transport. *Angew. Chem. Int. Ed.* **2019**, *58*, 15313–15317. [CrossRef]
14. Liu, T.Y.; Yuan, H.G.; Liu, Y.Y.; Ren, D.; Su, Y.C.; Wang, X. Metal-Organic Framework Nanocomposite Thin Films with Interfacial Bindings and Self-Standing Robustness for High Water Flux and Enhanced Ion Selectivity. *ACS Nano* **2018**, *12*, 9253–9265. [CrossRef]
15. De Luna, P.; Liang, W.; Mallick, A.; Shekhah, O.; García De Arquer, F.P.; Proppe, A.H.; Todorović, P.; Kelley, S.O.; Sargent, E.H.; Eddaoudi, M. Metal-Organic Framework Thin Films on High-Curvature Nanostructures Toward Tandem Electrocatalysis. *ACS Appl. Mater. Interfaces* **2018**, *10*, 31225–31232. [CrossRef]
16. Hoseini, S.J.; Bahrami, M.; Nabavizadeh, S.M. ZIF-8 Nanoparticles Thin Film at an Oil-Water Interface as an Electrocatalyst for the Methanol Oxidation Reaction without the Application of Noble Metals. *New J. Chem.* **2019**, *43*, 15811–15822. [CrossRef]
17. Fang, X.; Zong, B.; Mao, S. Metal–Organic Framework-Based Sensors for Environmental Contaminant Sensing. *Nano-Micro Lett.* **2018**, *10*, 64. [CrossRef] [PubMed]
18. Chocarro-Ruiz, B.; Pérez-Carvajal, J.; Avci, C.; Calvo-Lozano, O.; Alonso, M.I.; Maspoch, D.; Lechuga, L.M. A CO_2 Optical Sensor Based on Self-Assembled Metal-Organic Framework Nanoparticles. *J. Mater. Chem. A* **2018**, *6*, 13171–13177. [CrossRef]
19. Elmehrath, S.; Nguyen, H.L.; Karam, S.M.; Amin, A. BioMOF-Based Anti-Cancer Drug Delivery Systems. *Nanomaterials* **2023**, *13*, 953. [CrossRef]
20. Zhao, S.N.; Wang, G.; Poelman, D.; Van Der Voort, P. Luminescent Lanthanide MOFs: A Unique Platform for Chemical Sensing. *Materials* **2018**, *11*, 572. [CrossRef]
21. Liao, Z.; Xia, T.; Yu, E.; Cui, Y. Luminescent Metal–Organic Framework Thin Films: From Preparation to Biomedical Sensing Applications. *Crystals* **2018**, *8*, 338. [CrossRef]
22. Ramya, A.R.; Sharma, D.; Natarajan, S.; Reddy, M.L.P. Highly Luminescent and Thermally Stable Lanthanide Coordination Polymers Designed from 4-(Dipyridin-2-Yl)Aminobenzoate: Efficient Energy Transfer from Tb^{3+} to Eu^{3+} in a Mixed Lanthanide Coordination Compound. *Inorg. Chem.* **2012**, *51*, 8818–8826. [CrossRef]
23. Ramya, A.R.; Varughese, S.; Reddy, M.L.P. Tunable White-Light Emission from Mixed Lanthanide (Eu^{3+}, Gd^{3+}, Tb^{3+}) Coordination Polymers Derived from 4-(Dipyridin-2-Yl)Aminobenzoate. *Dalton Trans.* **2014**, *43*, 10940–10946. [CrossRef]
24. Zhang, R.; Zhu, L.; Yue, B. Luminescent Properties and Recent Progress in Applications of Lanthanide Metal-Organic Frameworks. *Chin. Chem. Lett.* **2023**, *34*, 108009. [CrossRef]
25. Gomez, G.E.; Roncaroli, F. Photofunctional Metal-Organic Framework Thin Films for Sensing, Catalysis and Device Fabrication. *Inorganica Chim. Acta* **2020**, *513*, 119926. [CrossRef]
26. Seethalekshmi, S.; Ramya, A.R.; Reddy, M.L.P.; Varughese, S. Lanthanide Complex-Derived White-Light Emitting Solids: A Survey on Design Strategies. *J. Photochem. Photobiol. C Photochem. Rev.* **2017**, *33*, 109–131. [CrossRef]
27. Tang, T.; Liu, M.; Chen, Z.; Wang, X.; Lai, C.; Ding, L.; Zeng, C. Highly Sensitive Luminescent Lanthanide Metal–Organic Framework Sensor for L-Kynurenine. *J. Rare Earths* **2022**, *40*, 415–420. [CrossRef]
28. Liu, W.; Li, D.; Wang, F.; Chen, X.; Wang, X.; Tian, Y. A Luminescent Lanthanide MOF as Highly Selective and Sensitive Fluorescent Probe for Nitrobenzene and Fe^{3+}. *Opt. Mater.* **2022**, *123*, 111895. [CrossRef]
29. Min, J.; Qu, X.L.; Yan, B. Tb Post-Functionalized La (III) Metal Organic Framework Hybrid Probe for Simple and Highly Sensitive Detection of Acetaldehyde. *Sens. Actuators B Chem.* **2019**, *300*, 126985. [CrossRef]
30. Li, C.; Zeng, C.; Chen, Z.; Jiang, Y.; Yao, H.; Yang, Y.; Wong, W.T. Luminescent Lanthanide Metal-Organic Framework Test Strip for Immediate Detection of Tetracycline Antibiotics in Water. *J. Hazard. Mater.* **2020**, *384*, 121498. [CrossRef] [PubMed]
31. Qu, X.L.; Yan, B. Ln(III)-Functionalized Metal-Organic Frameworks Hybrid System: Luminescence Properties and Sensor for Trans, Trans-Muconic Acid as a Biomarker of Benzene. *Inorg. Chem.* **2018**, *57*, 7815–7824. [CrossRef] [PubMed]

32. Zhao, Y.W.; Zhang, F.Q.; Zhang, X.M. Single Component Lanthanide Hybrids Based on Metal-Organic Framework for Near-Ultraviolet White Light LED. *ACS Appl. Mater. Interfaces* **2016**, *8*, 24123–24130. [CrossRef] [PubMed]
33. Wang, B.H.; Yan, B. Tunable Multi-Color Luminescence and White Emission in Lanthanide Ion Functionalized Polyoxometalate-Based Metal–Organic Frameworks Hybrids and Fabricated Thin Films. *J. Alloys Compd.* **2019**, *777*, 415–422. [CrossRef]
34. Wu, J.; Zhang, H.; Du, S. Tunable Luminescence and White Light Emission of Mixed Lanthanide-Organic Frameworks Based on Polycarboxylate Ligands. *J. Mater. Chem. C* **2016**, *4*, 3364–3374. [CrossRef]
35. Zhao, Y.; Li, D. Lanthanide-Functionalized Metal-Organic Frameworks as Ratiometric Luminescent Sensors. *J. Mater. Chem. C* **2020**, *8*, 12739–12754. [CrossRef]
36. Ji, G.; Liu, J.; Gao, X.; Sun, W.; Wang, J.; Zhao, S.; Liu, Z. A Luminescent Lanthanide MOF for Selectively and Ultra-High Sensitively Detecting Pb^{2+} Ions in Aqueous Solution. *J. Mater. Chem. A* **2017**, *5*, 10200–10205. [CrossRef]
37. Zhao, Y.; Wan, M.Y.; Bai, J.P.; Zeng, H.; Lu, W.; Li, D. PH-Modulated Luminescence Switching in a Eu-MOF: Rapid Detection of Acidic Amino Acids. *J. Mater. Chem. A* **2019**, *7*, 11127–11133. [CrossRef]
38. Wu, K.Y.; Qin, L.; Fan, C.; Cai, S.L.; Zhang, T.T.; Chen, W.H.; Tang, X.Y.; Chen, J.X. Sequential and Recyclable Sensing of Fe^{3+} and Ascorbic Acid in Water with a Terbium(Iii)-Based Metal-Organic Framework. *Dalton Trans.* **2019**, *48*, 8911–8919. [CrossRef] [PubMed]
39. Song, K.; Xiao, W.; He, M.; Yu, J.; Bai, Y.; Guan, Y. Optical Determination of Nitro Phenol via Ratiometric Emission from Tb:Eu-MOFs: Chemical Synthesis and Spectral Response. *J. Photochem. Photobiol. A Chem.* **2020**, *389*, 112194. [CrossRef]
40. Gao, Y.; Yu, G.; Liu, K.; Wang, B. Luminescent Mixed-Crystal Ln-MOF Thin Film for the Recognition and Detection of Pharmaceuticals. *Sens. Actuators B Chem.* **2018**, *257*, 931–935. [CrossRef]
41. Yang, X.; Lin, X.; Zhao, Y.; Zhao, Y.S.; Yan, D. Lanthanide Metal–Organic Framework Microrods: Colored Optical Waveguides and Chiral Polarized Emission. *Angew. Chem. Int. Ed.* **2017**, *56*, 7853–7857. [CrossRef]
42. Guo, H.; Wu, N.; Xue, R.; Liu, H.; Li, L.; Wang, M.-Y.; Yao, W.-Q.; Li, Q.; Yang, W. Multifunctional Ln-MOF Luminescent Probe Displaying Superior Capabilities for Highly Selective Sensing of Fe^{3+} and Al^{3+} Ions and Nitrotoluene. *Colloids Surf. A Physicochem. Eng. Asp.* **2020**, *585*, 124094. [CrossRef]
43. Tao, Y.; Zhang, P.; Liu, J.; Chen, X.; Guo, X.; Jin, H.; Chai, J.; Wang, L.; Fan, Y. Multi-Responsive Luminescent Sensor Based on Three Dimensional Lanthanide Metal-Organic Framework. *New J. Chem.* **2018**, *42*, 19485–19493. [CrossRef]
44. Wang, C.Y.; Wang, C.C.; Zhang, X.W.; Ren, X.Y.; Yu, B.; Wang, P.; Zhao, Z.X.; Fu, H. A New Eu-MOF for Ratiometrically Fluorescent Detection toward Quinolone Antibiotics and Selective Detection toward Tetracycline Antibiotics. *Chin. Chem. Lett.* **2022**, *33*, 1353–1357. [CrossRef]
45. Dou, Z.; Yu, J.; Xu, H.; Cui, Y.; Yang, Y.; Qian, G. Preparation and Thiols Sensing of Luminescent Metal-Organic Framework Films Functionalized with Lanthanide Ions. *Microporous Mesoporous Mater.* **2013**, *179*, 198–204. [CrossRef]
46. Liu, X.; Fu, W.; Bouwman, E. One-Step Growth of Lanthanoid Metal-Organic Framework (MOF) Films under Solvothermal Conditions for Temperature Sensing. *Chem. Commun.* **2016**, *52*, 6926–6929. [CrossRef]
47. Zhang, Y.; Lu, H.; Yan, B. Determination of Urinary N-Acetylneuraminic Acid for Early Diagnosis of Lung Cancer by a Boric Acid Covalently Functionalized Lanthanide MOFs and Its Intelligent Visual Molecular Robot Application. *Sens. Actuators B Chem.* **2021**, *349*, 130736. [CrossRef]
48. Balderas, J.U.; Navarro, D.; Vargas, V.; Tellez-Cruz, M.M.; Carmona, S.; Falcony, C. Ultrasonic Spray Deposition as a New Route to Luminescent MOF Film Synthesis. *J. Lumin.* **2019**, *212*, 322–327. [CrossRef]
49. Chernikova, V.; Shekhah, O.; Spanopoulos, I.; Trikalitis, P.N.; Eddaoudi, M. Liquid Phase Epitaxial Growth of Heterostructured Hierarchical MOF Thin Films. *Chem. Commun.* **2017**, *53*, 6191–6194. [CrossRef] [PubMed]
50. Mártire, A.P.; Segovia, G.M.; Azzaroni, O.; Rafti, M.; Marmisollé, W. Layer-by-Layer Integration of Conducting Polymers and Metal Organic Frameworks onto Electrode Surfaces: Enhancement of the Oxygen Reduction Reaction through Electrocatalytic Nanoarchitectonics. *Mol. Syst. Des. Eng.* **2019**, *4*, 893–900. [CrossRef]
51. Kim, K.J.; Zhang, Y.; Kreider, P.B.; Chong, X.; Wang, A.X.; Ohodnicki, P.R.; Baltrus, J.P.; Chang, C.H. Nucleation and Growth of Oriented Metal-Organic Framework Thin Films on Thermal SiO_2 Surface. *Thin Solid Film.* **2018**, *659*, 24–35. [CrossRef]
52. Huang, Y.; Tao, C.A.; Chen, R.; Sheng, L.; Wang, J. Comparison of Fabrication Methods of Metal-Organic Framework Optical Thin Films. *Nanomaterials* **2018**, *8*, 676. [CrossRef] [PubMed]
53. Shen, X.; Yan, B. Polymer Hybrid Thin Films Based on Rare Earth Ion-Functionalized MOF: Photoluminescence Tuning and Sensing as a Thermometer. *Dalton Trans.* **2015**, *44*, 1875–1881. [CrossRef]
54. Duan, T.W.; Yan, B. Hybrids Based on Lanthanide Ions Activated Yttrium Metal-Organic Frameworks: Functional Assembly, Polymer Film Preparation and Luminescence Tuning. *J. Mater. Chem. C* **2014**, *2*, 5098–5104. [CrossRef]
55. Gu, Z.G.; Chen, Z.; Fu, W.Q.; Wang, F.; Zhang, J. Liquid-Phase Epitaxy Effective Encapsulation of Lanthanide Coordination Compounds into MOF Film with Homogeneous and Tunable White-Light Emission. *ACS Appl. Mater. Interfaces* **2015**, *7*, 28585–28590. [CrossRef]
56. Zhang, Z.; Ma, W.; Yan, B. Multi-Step Tandem Functionalization Assembly of MOFs-Based Hybrid Polymeric Films for Color Tuning Luminescence and Responsive Sensing on Organic Vapors. *Colloids Surf. A Physicochem. Eng. Asp.* **2022**, *648*, 129416. [CrossRef]
57. Shekhah, O.; Liu, J.; Fischer, R.A.; Wöll, C. MOF Thin Films: Existing and Future Applications. *Chem. Soc. Rev.* **2011**, *40*, 1081–1106. [CrossRef] [PubMed]

58. Shi, X.; Shan, Y.; Du, M.; Pang, H. Synthesis and Application of Metal-Organic Framework Films. *Coord. Chem. Rev.* **2021**, *444*, 214060. [CrossRef]
59. Liu, J.; Wöll, C. Surface-Supported Metal-Organic Framework Thin Films: Fabrication Methods, Applications, and Challenges. *Chem. Soc. Rev.* **2017**, *46*, 5730–5770. [CrossRef] [PubMed]
60. Qiu, S.; Xue, M.; Zhu, G. Metal-Organic Framework Membranes: From Synthesis to Separation Application. *Chem. Soc. Rev.* **2014**, *43*, 6116–6140. [CrossRef]
61. Li, W. Metal–Organic Framework Membranes: Production, Modification, and Applications. *Prog. Mater. Sci.* **2019**, *100*, 21–63. [CrossRef]
62. Li, C.; Zhang, F.; Li, X.; Zhang, G.; Yang, Y. A Luminescent Ln-MOF Thin Film for Highly Selective Detection of Nitroimidazoles in Aqueous Solutions Based on Inner Filter Effect. *J. Lumin.* **2019**, *205*, 23–29. [CrossRef]
63. Ji, Y.; Qian, W.; Yu, Y.; An, Q.; Liu, L.; Zhou, Y.; Gao, C. Recent Developments in Nanofiltration Membranes Based on Nanomaterials. *Chin. J. Chem. Eng.* **2017**, *25*, 1639–1652. [CrossRef]
64. Sahoo, S.; Mondal, S.; Sarma, D. Luminescent Lanthanide Metal Organic Frameworks (LnMOFs): A Versatile Platform towards Organomolecule Sensing. *Coord. Chem. Rev.* **2022**, *470*, 214707. [CrossRef]
65. Crivello, C.; Sevim, S.; Graniel, O.; Franco, C.; Pane, S.; Puigmarti-Luis, J.; Munoz-Rojas, D. Advanced Technologies for the Fabrication of MOF Thin Films. *Mater. Horiz.* **2021**, *8*, 168–178. [CrossRef]
66. Jia, P.; Wang, Z.; Zhang, Y.; Zhang, D.; Gao, W.; Su, Y.; Li, Y.; Yang, C. Selective Sensing of Fe3+ Ions in Aqueous Solution by a Biodegradable Platform Based Lanthanide Metal Organic Framework. *Spectrochim. Acta Part A Mol. Biomol. Spectrosc.* **2020**, *230*, 118084. [CrossRef]
67. Wang, X.; Zhu, R.; Wang, X.; Liu, F.; Gao, Y.; Guan, R.; Chen, Y. Flexible and Washable CDs@Eu-MOFs/PVDF Multifunctional Thin Films as Highly Selective Sensing for Nitrobenzene and 4-Nitrophenol. *Inorg. Chem. Commun.* **2023**, *149*, 110423. [CrossRef]
68. Guo, H.; Zhu, Y.; Qiu, S.; Lercher, A.J.; Zhang, H. Coordination Modulation Induced Synthesis of Nanoscale Eu 1-Tbxmetal-Organic Frameworks for Luminescent Thin Films. *Adv. Mater.* **2010**, *22*, 4190–4192. [CrossRef]
69. Guo, H.; Zhu, S.; Cai, D.; Liu, C. Fabrication of ITO Glass Supported Tb-MOF Film for Sensing Organic Solvent. *Inorg. Chem. Commun.* **2014**, *41*, 29–32. [CrossRef]
70. Ozer, R.R.; Hinestroza, J.P. One-Step Growth of Isoreticular Luminescent Metal-Organic Frameworks on Cotton Fibers. *RSC Adv.* **2015**, *5*, 15198–15204. [CrossRef]
71. Brunckova, H.; Mudra, E.; Streckova, M.; Medvecky, L.; Sopcak, T.; Shepa, I.; Kovalcikova, A.; Lisnichuk, M.; Kolev, H. Transformation of Amorphous Terbium Metal–Organic Framework on Terbium Oxide TbOx(111) Thin Film on Pt(111) Substrate: Structure of TbxOy Film. *Nanomaterials* **2022**, *12*, 2817. [CrossRef]
72. Brunckova, H.; Mudra, E.; Rocha, L.; Nassar, E.; Nascimento, W.; Kolev, H.; Kovalcikova, A.; Molcanova, Z.; Podobova, M.; Medvecky, L. Preparation and Characterization of Isostructural Lanthanide Eu/Gd/Tb Metal-Organic Framework Thin Films for Luminescent Applications. *Appl. Surf. Sci.* **2021**, *542*, 148731. [CrossRef]
73. Zhang, J.; Xia, T.; Zhao, D.; Cui, Y.; Yang, Y.; Qian, G. In Situ Secondary Growth of Eu(III)-Organic Framework Film for Fluorescence Sensing of Sulfur Dioxide. *Sens. Actuators B Chem.* **2018**, *260*, 63–69. [CrossRef]
74. Cui, X.Y.; Gu, Z.Y.; Jiang, D.Q.; Li, Y.; Wang, H.F.; Yan, X.P. In Situ Hydrothermal Growth of Metal-Organic Framework 199 Films on Stainless Steel Fibers for Solid-Phase Microextraction of Gaseous Benzene Homologues. *Anal. Chem.* **2009**, *81*, 9771–9777. [CrossRef]
75. Luo, R.; Fu, H.; Li, Y.; Xing, Q.; Liang, G.; Bai, P.; Guo, X.; Lyu, J.; Tsapatsis, M. In Situ Fabrication of Metal–Organic Framework Thin Films with Enhanced Pervaporation Performance. *Adv. Funct. Mater.* **2023**, *33*, 2213221. [CrossRef]
76. Brunckova, H.; Mudra, E.; Rocha, L.; Nassar, E.; Nascimento, W.; Kolev, H.; Lisnichuk, M.; Kovalcikova, A.; Molcanova, Z.; Strečkova, M.; et al. Nanostructure and Luminescent Properties of Bimetallic Lanthanide Eu/Gd, Tb/Gd and Eu/Tb Coordination Polymers. *Inorganics* **2021**, *9*, 77. [CrossRef]
77. Shekhah, O. Layer-by-Layer Method for the Synthesis and Growth of Surface Mounted Metal-Organic Frameworks (SURMOFs). *Materials* **2010**, *3*, 1302–1315. [CrossRef]
78. Marets, N.; Kanno, S.; Ogata, S.; Ishii, A.; Kawaguchi, S.; Hasegawa, M. Lanthanide-Oligomeric Brush Films: From Luminescence Properties to Structure Resolution. *ACS Omega* **2019**, *4*, 15512–15520. [CrossRef]
79. Brower, L.J.; Gentry, L.K.; Napier, A.L.; Anderson, M.E. Tailoring the Nanoscale Morphology of HKUST-1 Thin Films via Codeposition and Seeded Growth. *Beilstein J. Nanotechnol.* **2017**, *8*, 2307–2314. [CrossRef]
80. Wang, Z.; Liu, J.; Arslan, H.K.; Grosjean, S.; Hagendorn, T.; Gliemann, H.; Bräse, S.; Wöll, C. Post-Synthetic Modification of Metal-Organic Framework Thin Films Using Click Chemistry: The Importance of Strained C-C Triple Bonds. *Langmuir* **2013**, *29*, 15958–15964. [CrossRef]
81. Wang, Y.; Zhang, G.; Zhang, F.; Chu, T.; Yang, Y. A Novel Lanthanide MOF Thin Film: The Highly Performance Self-Calibrating Luminescent Sensor for Detecting Formaldehyde as an Illegal Preservative in Aquatic Product. *Sens. Actuators B Chem.* **2017**, *251*, 667–673. [CrossRef]
82. Li, J.; Yuan, X.; Wu, Y.-N.; Ma, X.; Li, F.; Zhang, B.; Wang, Y.; Lei, Z.; Zhang, Z. From Powder to Cloth: Facile Fabrication of Dense MOF-76(Tb) Coating onto Natural Silk Fiber for Feasible Detection of Copper Ions. *Chem. Eng. J.* **2018**, *350*, 637–644. [CrossRef]

83. Chen, D.H.; Sedykh, A.E.; Gomez, G.E.; Neumeier, B.L.; Santos, J.C.C.; Gvilava, V.; Maile, R.; Feldmann, C.; WÖll, C.; Janiak, C.; et al. SURMOF Devices Based on Heteroepitaxial Architectures with White-Light Emission and Luminescent Thermal-Dependent Performance. *Adv. Mater. Interfaces* **2020**, *7*, 2000929. [CrossRef]
84. Chen, D.H.; Haldar, R.; Neumeier, B.L.; Fu, Z.H.; Feldmann, C.; Wöll, C.; Redel, E. Tunable Emission in Heteroepitaxial Ln-SURMOFs. *Adv. Funct. Mater.* **2019**, *29*, 1903086. [CrossRef]
85. Zhang, F.; Zhang, G.; Yao, H.; Wang, Y.; Chu, T.; Yang, Y. A Europium (III) Based Nano-Flake MOF Film for Efficient Fluorescent Sensing of Picric Acid. *Microchim. Acta* **2017**, *184*, 1207–1213. [CrossRef]
86. Zhang, F.; Wang, Y.; Chu, T.; Wang, Z.; Li, W.; Yang, Y. A Facile Fabrication of Electrodeposited Luminescent MOF Thin Films for Selective and Recyclable Sensing of Nitroaromatic Explosives. *Analyst* **2016**, *141*, 4502–4510. [CrossRef] [PubMed]
87. Wang, Z.; Liu, H.; Wang, S.; Rao, Z.; Yang, Y. A Luminescent Terbium-Succinate MOF Thin Film Fabricated by Electrodeposition for Sensing of Cu^{2+} in Aqueous Environment. *Sens. Actuators B Chem.* **2015**, *220*, 779–787. [CrossRef]
88. Li, W.J.; Feng, J.F.; Lin, Z.J.; Yang, Y.L.; Yang, Y.; Wang, X.S.; Gao, S.Y.; Cao, R. Patterned Growth of Luminescent Metal-Organic Framework Films: A Versatile Electrochemically-Assisted Microwave Deposition Method. *Chem. Commun.* **2016**, *52*, 3951–3954. [CrossRef]
89. Feng, J.F.; Yang, X.; Gao, S.Y.; Shi, J.; Cao, R. Facile and Rapid Growth of Nanostructured Ln-BTC Metal-Organic Framework Films by Electrophoretic Deposition for Explosives Sensing in Gas and Cr^{3+} Detection in Solution. *Langmuir* **2017**, *33*, 14238–14243. [CrossRef] [PubMed]
90. Jia, Z.; Hao, S.; Wen, J.; Li, S.; Peng, W.; Huang, R.; Xu, X. Electrochemical Fabrication of Metal–Organic Frameworks Membranes and Films: A Review. *Microporous Mesoporous Mater.* **2020**, *305*, 110322. [CrossRef]
91. Li, W.J.; Tu, M.; Cao, R.; Fischer, R.A. Metal-Organic Framework Thin Films: Electrochemical Fabrication Techniques and Corresponding Applications & Perspectives. *J. Mater. Chem. A* **2016**, *4*, 12356–12369. [CrossRef]
92. Zhang, X.; Wan, K.; Subramanian, P.; Xu, M.; Luo, J.; Fransaer, J. Electrochemical Deposition of Metal-Organic Framework Films and Their Applications. *J. Mater. Chem. A* **2020**, *8*, 7569–7587. [CrossRef]
93. Wang, Y.; Chu, T.; Yu, M.; Liu, H.; Yang, Y. One Step Cathodically Electrodeposited $[Tb_2(BDC)_3(H_2O)_4]_n$ Thin Film as a Luminescent Probe for Cu^{2+} Detection. *RSC Adv.* **2014**, *4*, 58178–58183. [CrossRef]
94. Liu, H.; Wang, H.; Chu, T.; Yu, M.; Yang, Y. An Electrodeposited Lanthanide MOF Thin Film as a Luminescent Sensor for Carbonate Detection in Aqueous Solution. *J. Mater. Chem. C* **2014**, *2*, 8683–8690. [CrossRef]
95. Liu, H.; Chu, T.; Rao, Z.; Wang, S.; Yang, Y.; Wong, W.T. The Tunable White-Light and Multicolor Emission in An Electrodeposited Thin Film of Mixed Lanthanide Coordination Polymers. *Adv. Opt. Mater.* **2015**, *3*, 1545–1550. [CrossRef]
96. Alizadeh, S.; Nematollahi, D. Convergent and Divergent Paired Electrodeposition of Metal-Organic Framework Thin Films. *Sci. Rep.* **2019**, *9*, 14325. [CrossRef]
97. Hauser, J.L.; Tso, M.; Fitchmun, K.; Oliver, S.R.J. Anodic Electrodeposition of Several Metal Organic Framework Thin Films on Indium Tin Oxide Glass. *Cryst. Growth Des.* **2019**, *19*, 2358–2365. [CrossRef]
98. Li, W.J.; Lü, J.; Gao, S.Y.; Li, Q.H.; Cao, R. Electrochemical Preparation of Metal-Organic Framework Films for Fast Detection of Nitro Explosives. *J. Mater. Chem. A* **2014**, *2*, 19473–19478. [CrossRef]
99. Hod, I.; Bury, W.; Karlin, D.M.; Deria, P.; Kung, C.W.; Katz, M.J.; So, M.; Klahr, B.; Jin, D.; Chung, Y.W.; et al. Directed Growth of Electroactive Metal-Organic Framework Thin Films Using Electrophoretic Deposition. *Adv. Mater.* **2014**, *26*, 6295–6300. [CrossRef] [PubMed]
100. Feng, J.F.; Gao, S.Y.; Shi, J.; Liu, T.F.; Cao, R. C-QDs@UiO-66-$(COOH)_2$ Composite Film via Electrophoretic Deposition for Temperature Sensing. *Inorg. Chem.* **2018**, *57*, 2447–2454. [CrossRef] [PubMed]
101. Zhu, H.; Liu, H.; Zhitomirsky, I.; Zhu, S. Preparation of Metal-Organic Framework Films by Electrophoretic Deposition Method. *Mater. Lett.* **2015**, *142*, 19–22. [CrossRef]
102. Feng, J.F.; Gao, S.Y.; Liu, T.F.; Shi, J.; Cao, R. Preparation of Dual-Emitting Ln@UiO-66-Hybrid Films via Electrophoretic Deposition for Ratiometric Temperature Sensing. *ACS Appl. Mater. Interfaces* **2018**, *10*, 6014–6023. [CrossRef]
103. Aceituno Melgar, V.M.; Kwon, H.T.; Kim, J. Direct Spraying Approach for Synthesis of ZIF-7 Membranes by Electrospray Deposition. *J. Memb. Sci.* **2014**, *459*, 190–196. [CrossRef]
104. Bai, X.J.; Chen, D.; Li, L.L.; Shao, L.; He, W.X.; Chen, H.; Li, Y.N.; Zhang, X.M.; Zhang, L.Y.; Wang, T.Q.; et al. Fabrication of MOF Thin Films at Miscible Liquid-Liquid Interface by Spray Method. *ACS Appl. Mater. Interfaces* **2018**, *10*, 25960–25966. [CrossRef]
105. Li, Y.N.; Wang, S.; Zhou, Y.; Bai, X.J.; Song, G.S.; Zhao, X.Y.; Wang, T.Q.; Qi, X.; Zhang, X.M.; Fu, Y. Fabrication of Metal-Organic Framework and Infinite Coordination Polymer Nanosheets by the Spray Technique. *Langmuir* **2017**, *33*, 1060–1065. [CrossRef]
106. Giedraityte, Z.; Sundberg, P.; Karppinen, M. Flexible Inorganic-Organic Thin Film Phosphors by ALD/MLD. *J. Mater. Chem. C* **2015**, *3*, 12316–12321. [CrossRef]
107. Silva, R.M.; Carlos, L.D.; Rocha, J.; Silva, R.F. Luminescent Thin Films of Eu-Bearing UiO-66 Metal Organic Framework Prepared by ALD/MLD. *Appl. Surf. Sci.* **2020**, *527*, 146603. [CrossRef]
108. Feng, J.F.; Liu, T.F.; Shi, J.; Gao, S.Y.; Cao, R. Dual-Emitting UiO-66(Zr&Eu) Metal-Organic Framework Films for Ratiometric Temperature Sensing. *ACS Appl. Mater. Interfaces* **2018**, *10*, 20854–20861. [CrossRef] [PubMed]
109. Yang, D.; Wang, Y.; Liu, D.; Li, Z.; Li, H. Luminescence Modulation: Via Cation-π Interaction in a Lanthanide Assembly: Implications for Potassium Detection. *J. Mater. Chem. C* **2018**, *6*, 1944–1950. [CrossRef]

110. Yang, D.; Liu, D.; Tian, C.; Wang, S.; Li, H. Flexible and Transparent Films Consisting of Lanthanide Complexes for Ratiometric Luminescence Thermometry. *J. Colloid Interface Sci.* **2018**, *519*, 11–17. [CrossRef] [PubMed]
111. Mi, X.; Sheng, D.; Yu, Y.; Wang, Y.; Zhao, L.; Lu, J.; Li, Y.; Li, D.; Dou, J.; Duan, J.; et al. Tunable Light Emission and Multiresponsive Luminescent Sensitivities in Aqueous Solutions of Two Series of Lanthanide Metal-Organic Frameworks Based on Structurally Related Ligands. *ACS Appl. Mater. Interfaces* **2019**, *11*, 7914–7926. [CrossRef]
112. Bai, K.P.; Zhou, L.J.; Yang, G.P.; Cao, M.X.; Wang, Y.Y. Luminescence Sensing of Fe3+ and Nitrobenzene by Three Isostructural Ln–MOFs Assembled by a Phenyl-Dicarboxylate Ligand. *ChemistrySelect* **2019**, *4*, 12794–12800. [CrossRef]
113. Xu, J.; Jia, L.; Jin, N.; Ma, Y.; Liu, X.; Wu, W.; Liu, W.; Tang, Y.; Zhou, F. Fixed-Component Lanthanide-Hybrid-Fabricated Full-Color Photoluminescent Films as Vapoluminescent Sensors. *Chem. A Eur. J.* **2013**, *19*, 4556–4562. [CrossRef] [PubMed]
114. Chen, W.; Fan, R.; Fan, J.; Liu, H.; Sun, T.; Wang, P.; Yang, Y. Lanthanide Coordination Polymer-Based Composite Films for Selective and Highly Sensitive Detection of $Cr_2O_7^{2-}$ in Aqueous Media. *Inorg. Chem.* **2019**, *58*, 15118–15125. [CrossRef] [PubMed]
115. Xu, W.; Chen, H.; Xia, Z.; Ren, C.; Han, J.; Sun, W.; Wei, Q.; Xie, G.; Chen, S. A Robust TbIII-MOF for Ultrasensitive Detection of Trinitrophenol: Matched Channel Dimensions and Strong Host-Guest Interactions. *Inorg. Chem.* **2019**, *58*, 8198–8207. [CrossRef]
116. Zhu, Y.M.; Zeng, C.H.; Chu, T.S.; Wang, H.M.; Yang, Y.Y.; Tong, Y.X.; Su, C.Y.; Wong, W.T. A Novel Highly Luminescent LnMOF Film: A Convenient Sensor for Hg^{2+} Detecting. *J. Mater. Chem. A* **2013**, *1*, 11312–11319. [CrossRef]
117. Ma, W.P.; Yan, B. Lanthanide Functionalized MOF Thin Films as Effective Luminescent Materials and Chemical Sensors for Ammonia. *Dalton Trans.* **2020**, *49*, 15663–15671. [CrossRef] [PubMed]
118. Campagnol, N.; Rezende Souza, E.; De Vos, D.E.; Binnemans, K.; Fransaer, J. Luminescent Terbium-Containing Metal–Organic Framework Films: New Approaches for the Electrochemical Synthesis and Application as Detectors for Explosives. *Chem. Commun.* **2014**, *50*, 12680–12683. [CrossRef]
119. Wang, X.; Batra, K.; Clavier, G.; Maurin, G.; Ding, B.; Tissot, A.; Serre, C. Ln-MOF Based Ratiometric Luminescent Sensor for the Detection of Potential COVID-19 Drugs. *Chem. A Eur. J.* **2023**, *29*, e202203136. [CrossRef]
120. Feng, T.; Ye, Y.; Liu, X.; Cui, H.; Li, Z.; Zhang, Y.; Liang, B.; Li, H.; Chen, B. A Robust Mixed-Lanthanide PolyMOF Membrane for Ratiometric Temperature Sensing. *Angew. Chem. Int. Ed.* **2020**, *59*, 21752–21757. [CrossRef]
121. Wang, Y.; Xia, J.; Gao, Y. Decoding and Quantitative Detection of Antibiotics by a Luminescent Mixed-Lanthanide-Organic Framework. *Front. Environ. Sci. Eng.* **2022**, *16*, 154. [CrossRef]
122. Zhang, F.; Yao, H.; Chu, T.; Zhang, G.; Wang, Y.; Yang, Y. A Lanthanide MOF Thin-Film Fixed with Co_3O_4 Nano-Anchors as a Highly Efficient Luminescent Sensor for Nitrofuran Antibiotics. *Chem. A Eur. J.* **2017**, *23*, 10293–10300. [CrossRef] [PubMed]
123. Li, Y.; Sun, M.; Yang, Y.; Meng, H.; Wang, Q.; Li, C.; Li, G. Luminescence-Colour-Changing Sensing toward Neurological Drug Carbamazepine in Water and Biofluids Based on White Light-Emitting CD/Ln-MOF/PVA Test Papers. *J. Mater. Chem. C* **2021**, *9*, 8683–8693. [CrossRef]
124. Dong, J.; Zhao, D.; Lu, Y.; Sun, W.Y. Photoluminescent Metal-Organic Frameworks and Their Application for Sensing Biomolecules. *J. Mater. Chem. A* **2019**, *7*, 22744–22767. [CrossRef]
125. Simões, R.; Rodrigues, J.; Granadeiro, C.M.; Rino, L.; Neto, V.; Monteiro, T.; Gonçalves, G. Boosting the Optical Properties of Polylactic Acid/ Lanthanide-Based Metal-Organic Framework Composites. *Mater. Today Chem.* **2023**, *29*, 101436. [CrossRef]